ORIGINAL CONTRIBUTION

# Onset of entanglement and reptation in melts of linear homopolymers: consistent rheological simulations of experiments from oligomers to high polymers

**Fabio Zulli · Marco Giordano · Laura Andreozzi**

**Abstract** The shear rheological behavior is investigated in this work for a series of poly(ethyl acrylate) samples, whose molar mass ranges from oligomers to high polymers. The focus was on studying the onset of entanglement effects over selected reptation models in order to ascertain their ability to reproduce the complex shear modulus of the polymers and to provide consistent values of the microscopic parameters driving the structural relaxation of the polymer system. Among ordinary reptation topological models, we found that the Doi–Edward model, implemented with contour length fluctuation and constraint release mechanism for the tube relaxation, better reproduced the rheological response of the materials. Most importantly, we were able to simulate material functions to obtain consistent microscopic information on the materials, such as Rouse time and entanglement molar mass, over the whole range of investigated molar masses, therefore overcoming the discrepancy usually found, mostly in the mass region of partial entanglement. Finally, descriptions of the polymer entanglement features, in agreement with the experimental and microscopic model findings, are provided in the framework of the packing-length phenomenological model and by means of analytical calculations of the polymer viscosity according to the Milner–McLeish–Likhtman model.

F. Zulli · M. Giordano · L. Andreozzi (✉)
Department of Physics "E. Fermi", University of Pisa,
Largo B. Pontecorvo 3, 56127 Pisa, Italy
e-mail: laura.andreozzi@df.unipi.it

F. Zulli · M. Giordano · L. Andreozzi
UOS di Pisa, IPCF-CNR, Via G. Moruzzi 1, 56124 Pisa, Italy
e-mail: laura.andreozzi@df.unipi.it

## Introduction

Nowadays, predictions on the rheological behavior of polymer melts start from the Rouse model (Rouse 1953), well established for the long-time diffusion of low molecular weight polymer melts, and proceed to include dynamics processes that arise with the increasing of the polymer molar mass (Larson et al. 2007). In particular, it has been recognized that the chain entanglement is a salient feature in polymers, producing the viscoelastic polymer response and affecting flow behavior of polymer melts and solutions, and mechanical properties as well (Doi and Edwards 1988).

Dynamics of melts of high polymers and their concentrated solutions is prominently described by the tube models (Doi and Edwards 1988; de Gennes 1971). Accordingly, a topological restriction to molecular motion (entanglement) arises because of the presence of other chains. The entanglements confine the polymer chain motion to a tube. Since polymer chains would have be broken to allow the restricted chain to pass through them, chain diffusion induces the chain to flow outside the tube in a snake-like way (reptation). While tube models provide a plausible mechanism for the relaxation of polymers via reptation, the concept of tube that constrains the polymer motion is ill defined and elusive (for a very recent attempt to quantify the tube concept, see Likhtman 2014). Moreover, tube theories foresee scaling laws with respect to the polymer mass from which experiments deviate. Therefore, over the years, several models have been developed that implement reptation with more relaxation mechanisms, such as tube length fluctuations and

constraint release relaxation, and that also refine mixing rules in order to obtain quantitative predictions of linear viscoelasticity of polymer melts from the knowledge of molar mass distribution (Carrot and Guillet 1997; des Cloizeaux 1990; 1992; Léonardi et al. 2000; Likhtman and McLeish 2002; Pattamaprom et al. 2000; Thimm et al. 2000; van Ruymbeke et al. 2002). Also, many studies attempted to answer the question of the best overall model for the melt dynamics of well-entangled linear polymers (Carrot and Guillet 1997; des Cloizeaux 1990; 1992; Léonardi et al. 2000; Likhtman and McLeish 2002; Pattamaprom et al. 2000; Thimm et al. 2000; van Ruymbeke et al. 2002).

The tube theory of polymer dynamics relates the onset of entanglement to the entanglement mass $M_e$, which is the mass of a strand between neighboring entanglement points and is the fundamental topological input parameter of the theory. $M_e$, in turn, is related to the plateau modulus $G_N^0$ (Larson et al. 2003), as explicitly recalled later in this work, so that the value of $M_e$ could be conveniently estimated by measurements of the experimental elastic modulus $G$. However, recognizable effects of the polymer entanglement appear in the rubbery plateau of the experimental storage modulus for molar masses greater than $2M_e$, and, in addition, fluctuations have been reported in the literature for the experimental $G_N^0$ values of the same polymer matrix (Liu et al. 2006 and references therein).

It appears therefore of interest to investigate the onset and the presence of entanglement by studying the rheological response of a same narrowly distributed linear homopolymer as a function of its increasing mass from oligomer to high polymer, including the slightly entangled masses. This last range, characterized by molar masses greater than the entanglement mass $M_e$ and smaller than $2M_e$, has not been widely investigated yet, although the study of the viscoelasticity of slightly entangled polymers, as well as unentangled ones, deserves particular attention because it could allow the focusing on the onset of entanglement itself.

In this work, the complex shear modulus of poly(ethyl acrylate) (PEA) melts is predicted according to four models based on reptation. Since the molar mass of the samples ranges from oligomers to high polymers with about $15M_e$, indication could be inferred on the mass where the entanglement is expected to onset and its influence for a correct calculation of the experimental master curves (Andreozzi et al. 2013; Lin and Juang 1999).

Indeed, special care has been devoted to simulate in a consistent way the rheological response at the different masses. In particular, relaxation mechanisms and mixing rules were carefully taken into account so that consistent values of the common parameters, pertinent to the same relaxation mechanisms at the different masses, are obtained. To the aim, an isofrictional correction (Andreozzi et al.

2008; Colby et al. 1987) is adopted to consider the different free volume amount at the chain-ends of the lightest samples. Moreover, the role of contour length fluctuation and constraint release relaxation is discussed.

The $M_e$ datum obtained from calculations of PEA master curves has been used to test the packing model (Fetters et al. 1994; Fetters et al. 1999), an empirical model, widely employed in the literature, that relates viscoelastic properties to the chain dimensions. The insertion of PEA in the framework of the packing model confirmed the possibility of describing the dynamics of these homopolymers in terms of their conformation properties, as recently demonstrated also in case of a series of methacrylate liquid crystalline copolymers (Andreozzi et al. 2013).

The analysis of reptation dynamics was completed using the Milner–McLeish–Likhtman model (Likhtman and McLeish 2002) to calculate viscosity of PEAs. The predictive ability of the model was confirmed by the resulting evaluation of entanglement-related material parameters such as reptation mass and critical mass for PEAs.

## Theoretical background

In this paper, the complex shear modulus of the series of PEA polymer melts was calculated, considering different models and mechanisms for relaxation, including Rouse model, Doi–Edwards theory for entanglement polymer dynamics, contour length fluctuation, and constraint release relaxation (Doi and Edwards 1988). The discussion also includes data treatment according to Milner–McLeish–Likhtman model (Likhtman and McLeish 2002). In the following, only the results of the models relevant to the present work are reported. More details can be found in literature (des Cloizeaux 1988; Doi and Edwards 1988; Graessley 1982; Ianniruberto and Marrucci 1996; Larson et al. 2003; Marrucci 1985; Milner and McLeish 1998; Pattamaprom et al. 2000; Rubinstein et al. 1987; Rubinstein and Colby 1988; Tsenoglou 1991; Viovy et al. 1991).

According to the Rouse theory for unentangled chains (UR), the shear relaxation modulus of a monodisperse melt, with molar mass $M$ and at temperature $T$, can be written as a function of the time $t$ as (Doi and Edwards 1988)

$$G(t) = \frac{\rho N_A k_B T}{M} \sum_{p>0} \exp\left(-2\frac{p^2 t}{\tau_R}\right) = \frac{\rho N_A k_B T}{M} m_{UR}(t)$$

(1)

In Eq. 1, $m_{UR}(t)$ is the relaxation function, $\rho$ the density of the melt, $N_A$ is the Avogadro number, $k_B$ the Boltzmann constant, and $\tau_R$ is the Rouse relaxation time, which, in turn, depends on the monomeric friction coefficient $\zeta_0$, the length

$b$ and the number $N$ of chain segments according to (Doi and Edwards 1988)

$$\tau_R = \frac{\zeta_0 N^2 b^2}{3\pi^2 k_B T} = K_R N^2 \qquad (2)$$

In Eq. 2, $K_R$ is a parameter independent of the molar mass $M$ (i.e., $N$).

When the macromolecules in the melt are not constrained by entanglements ($M < M_e$), the relaxation results from monomer friction only and is described by the Rouse mechanism. Also in entangled polymers, the relaxation processes are dominated by the Rouse mechanism (Doi and Edwards 1988) at a time much shorter than a characteristic time for reptation and named reptation time. However, a significant difference is found for the Rouse relaxation of entangled polymer melts with respect to the unentangled ones: at times about the entanglement time[1] $\tau_e = \tau_R M_e^2/M^2$ (Larson et al. 2003) or greater, those modes given by sub-chains with molar mass lower than $M_e$ are relaxed, while the Rouse relaxation of longer modes/sub-chains is hampered by the presence of the reptation tube (van Ruymbeke et al. 2002; Likhtman and McLeish 2002; Léonardi et al. 2000; Carrot and Guillet 1997), so that only longitudinal Rouse modes along the tube contribute to the relaxation. This leads to (Likhtman and McLeish 2002)

$$G(t) = \frac{\rho N_A k_B T}{M} \sum_{p > M/M_e} \exp\left(-2\frac{p^2 t}{\tau_R}\right) \qquad (3)$$
$$+ \kappa \frac{\rho N_A k_B T}{M} \sum_{p=1}^{M/M_e} \exp\left(-\frac{p^2 t}{\tau_R}\right) = \frac{\rho N_A k_B T}{M} m_{ER}(t)$$

where $m_{ER}(t)$ is the relaxation function of the Rouse modes in entangled chains (ER).

The Rouse mechanism of relaxation of unentangled sub-chains (fast modes with $p > M/M_e$ inside the tube) and the relaxation of the slower longitudinal modes are combined in Eq. 3. For the latter, in some studies (Milner and McLeish 1998; Pattamaprom et al. 2000; van Ruymbeke et al. 2002), the empirical factor $\kappa = 1/3$ was used to account for that only one mode over three takes part in the relaxation. Other studies (Likhtman and McLeish 2002) provided the different value $\kappa = 1/5$. This means that 1/5 of the stress stored in the tube is relaxed after a time $\tau_R$ by longitudinal modes. At $\tau_R$, the residual fraction of the stress is therefore supplied by unrelaxed mechanisms, such as reptative relaxations. In this paper, we will refer to the model of Eq. 3 as ER3 or ER5 depending on the value employed for $\kappa$ 1/3 or 1/5, respectively.

---

[1] In this paper, we follow the "G" convention for the definitions of entanglement spacing and time constants in the tube model treated extensively in Larson et al. (2003).

Several models have been proposed in the literature to describe the reptative dynamics of entangled linear chains. According to the first quantitative description by Doi and Edwards (1988), the shear stress modulus in entangled chains (DE) can be expressed as

$$G(t) = \frac{\rho N_A k_B T}{M_e} \frac{8}{\pi^2} \sum_{p:\text{ odd}} \exp\left(-\frac{p^2 t}{\tau_d}\right) = G_N^0 \, m_{DE}(t) \qquad (4)$$

In Eq. 4, $G_N^0$ is the plateau modulus, $m_{DE}(t)$ the relaxation function. $\tau_d$ is the disengagement time, or reptation time, and is the time for the chain to renew its configuration and to escape from the tube. $\tau_d$ is also the longest relaxation time of the polymer melt. It is given by (Larson et al. 2003)

$$\tau_d = \frac{\zeta_0 N^3 b^4}{\pi^2 k_B T a^2} = 3\frac{N b^2}{a^2} \tau_R = 3\frac{M}{M_e} \tau_R \qquad (5)$$

where $a$ is the tube diameter.

It is seen from Eq. 5 that DE model yields $\tau_d \sim M^3$, which is not equal, but quite close, to the experimental result of $\tau_d \sim M^{3.4}$. As a matter of fact, the empirical expression for the disengagement time

$$\tau_d = K_d \, (M/M_e)^\alpha \qquad (6)$$

is often used that forces the exponent value to $\alpha = 3.4$. In Eq. 6, $K_d$ is a proper temperature-dependent factor (van Ruymbeke et al. 2002).

In order to recover the $\tau_d \sim M^{3.4}$ experimental dependence of the entangled polymer melts from the theory, the DE relaxation function can be modified to include fluctuations of the tube length around its equilibrium value. This leads to an expression for $G(t)$ (DECLF) (Doi and Edwards 1988; van Ruymbeke et al. 2002; Likhtman and McLeish 2002) in terms of the fractional distance $\xi$ of tube segments from the end of the tube at the time $t = 0$

$$G(t) = \frac{\rho N_A k_B T}{M_e} \int_0^1 \exp\left(-\frac{t}{\tau(\xi)}\right) d\xi = G_N^0 \, m_{DECLF}(t) \qquad (7a)$$

with

$$\tau(\xi) = \frac{\xi^4}{4\xi_{cr}^4} \tau_d \qquad 0 < \xi < \xi_{cr} \qquad (7b)$$

$$\tau(\xi) = \left(\xi - \frac{\xi_{cr}}{2}\right)^2 \tau_d \qquad \xi_{cr} < \xi < 1 \qquad (7c)$$

$$\xi_{cr} = 2v\sqrt{\frac{M_e}{M}} \qquad (7d)$$

that is just constructed to merge the fluctuations at short time scale with the reptation at long times, discriminated by $\xi_{cr}$ (Doi and Edwards 1988). Equation 7d expresses $\xi_{cr}$ in terms of the molar mass, the entanglement mass, and the parameter $\upsilon$ that depends on the material (van Ruymbeke et al. 2002).

The contour length fluctuations are also semi-empirically accounted for by another development of the DE theory, the time-dependent diffusion model (TDD), which provides (des Cloizeaux 1988)

$$G(t) = \frac{\rho N_A k_B T}{M_e} \frac{8}{\pi^2} \sum_{p:\text{ odd}} \frac{1}{p^2} e^{-p^2\left(\frac{t}{\tau_d} - \frac{M_d}{M} g\left(\frac{Mt}{M_d \tau_d}\right)\right)}$$

$$= G_N^0 \; m_{\text{TDD}}(t) \qquad (8)$$

In this formula, $m_{\text{TDD}}(t)$ is the TDD relaxation function, $M_d$ is an empirical parameter and $g$ is defined according to des Cloizeaux (1988)

$$g(x) = \sum_{k>0} \frac{1 - e^{-kx^2}}{k^2} \approx -x + \sqrt{x^2 + \sqrt{\pi x^3} + \pi x} \qquad (9)$$

As a general remark, the tube model assumes an immobile tube. Indeed, this assumption is an oversimplification: the tube constraints are themselves chains that are also reptating, having therefore a finite lifetime. The constraint release (CR) mechanism overcomes this drawback of the tube model and can be included as a relaxation way for the chains, applying the double reptation scheme (des Cloizeaux 1988; Graessley 1982) to the DE, DECLF, and TDD models. The semi-empirical approach of double reptation explicitly describes entanglements as binary events (des Cloizeaux 1988; Graessley 1982). The intuitive idea behind it is that an entanglement disappears, and hence a constraint is released, whenever a chain end passes beyond the entanglement. For monodisperse polymer melts, the stress relaxation function within the double reptation theory is proportional to the square of $m(t)$ according to (des Cloizeaux 1988; Tsenoglou 1987)

$$G_{\text{double}}(t) = G_N^0 \; m_{\text{single}}^2(t) \qquad (10)$$

where $m_{\text{single}}(t)$ is the shear modulus relaxation function of single reptation models without the CR mechanism (e.g., Eqs. 4, 7, and 8).

Then, the total shear relaxation modulus $G(t)$ of the monodisperse polymer melt can be obtained as a sum of the different contributions chosen to model the relaxation:

$$G(t, M) = G_N^0 \; m_{\text{single}}^\beta(t, M) + \frac{\rho N_A k_B T}{M} m_{\text{Rouse}}(t, M)$$
$$(11)$$

The exponent $\beta$ accounts for the CR mechanism, $m_{\text{single}}(t, M)$ is the shear modulus relaxation function of single reptation models of the monodisperse polymer of mass $M$, as for Eq. 10. The $m_{\text{Rouse}}(t, M)$ provides the Rouse relaxation of the polymer chains and corresponds to $m_{\text{ER}}(t)$ or $m_{\text{UR}}(t)$ for entangled or unentangled chains, respectively.

A further model was proposed in the literature, which combines self-consistently theories for contour length fluctuations and CR mechanism: the Milner–McLeish–Likhtman (MML) model (Likhtman and McLeish 2002). This model starts from the DE model and unites theoretical and stochastic simulation approaches, adopting a renormalization of the disengagement time to include contour length fluctuation, while CR mechanism is added following a scheme proposed by Rubinstein and Colby (1988) and Viovy et al. (1991).

With reference to Eq. 11, $\beta$ is always set to 1 in the MML model and the reptative contribution to $G(t)$ is given by (Likhtman and McLeish 2002):

$$G(t) = G_N^0 \; R(t, c_v) \; s(t) = G_N^0 \; m_{\text{MML}}(t) \qquad (12)$$

where $m_{\text{MML}} = m_{\text{single}}(t, M)$ is the shear modulus relaxation function of the MML model, $s(t)$ is an occupation function accounting for the fraction of tube segment not visited by a chain end during the time $t$, and $R(t, c_v)$ is the relaxation function of the tube. The dimensionless parameter $c_v$ reflects the "strength" of the CR mechanism, so that the value $c_v = 0$ means no CR, while $c_v = 1$ corresponds to the Rubinstein–Colby theory (Rubinstein and Colby 1988; Viovy et al. 1991). Details about the determination of $R(t, c_v)$ are given in Likhtman and McLeish (2002), where an important role is also played by the knowledge of $b$.

By means of fitting the results of stochastic simulations, MML model provides for $s(t)$

$$s(t) = \widetilde{G}_f \frac{8}{\pi^2} \sum_{p:\text{ odd}}^{\sqrt{Z/10}} \frac{1}{p^2} \exp\left(-\frac{p^2 t}{\widetilde{\tau}_f}\right)$$

$$+ \int_{\widetilde{\varepsilon}_f}^{\infty} \frac{0.306}{Z \tau_e^{1/4} \varepsilon^{5/4}} e^{-\varepsilon t} \, d\varepsilon \qquad (13a)$$

where the factor 0.306 was adopted to reproduce the early time value, when relaxation process of tube segments is strongly non-exponential, $Z = M/M_e$ and

$$\frac{\widetilde{\tau}_f}{\tau_d} = 1 - 2\frac{1.69}{Z^{1/2}} + \frac{4.17}{Z} - \frac{1.55}{Z^{3/2}} \qquad (13b)$$

$$\widetilde{G} = 1 - \frac{1.69}{Z^{1/2}} + \frac{2.00}{Z} - \frac{1.24}{Z^{3/2}} \qquad (13c)$$

$$\widetilde{\varepsilon}_f = \frac{1}{\tau_e} \left( \frac{4 \times 0.306}{Z} \right)^4 \left( 1 - \widetilde{G}_f \frac{8}{\pi^2} \sum_{p:\,\text{odd}}^{\sqrt{Z/10}} \frac{1}{p^2} \right)^{-4} \quad (13\text{d})$$

The last equation is set by the condition $s(0) = 1$.

Polydisperse polymers can be profitably handled taking into account the contributions to $G(t, M)$ of all monodisperse components of mass $M$ of the molar mass distribution $w(M)$ of the melt

$$w(M) = \frac{\mathrm{d}W(M)}{\mathrm{d}\log M} \quad (14)$$

where $W(M)$ is the weight fraction of chains with molar mass lower than $M$. Accordingly, the overall relaxation modulus of polydisperse polymers can be written in the general mixing rule form (Tsenoglou 1991; van Ruymbeke et al. 2002)

$$G(t) = G_N^0 \left( \int_{\log M_i}^{\log M_f} m_{\text{single}}(t, M) w(M) \, \mathrm{d}\log M \right)^\beta$$
$$+ \frac{\rho N_A k_B T}{M} \int_{\log M_i}^{\log M_f} m_{\text{Rouse}}(t, M) w(M) \, \mathrm{d}\log M \quad (15)$$

where $m_{\text{single}}(t, M)$ and $m_{\text{Rouse}}(t, M)$ are the relaxation functions of the monodisperse polymer of mass $M$. The values of the extremes of the molar mass range ($M_i$ and $M_f$) and the value of the exponent $\beta > 0$ are specific to the model describing the monodisperse shear modulus and relaxation function, as detailed in Table 1. In particular, $\beta$ is a dumb parameter for MML model and has to be set to 1, because CR mechanism is controlled by $c_v$. Note that, in the absence of CR mechanism, namely $\beta = 1$ (and also $c_v = 0$ for MML model), one could obtain $G^*(\omega)$ from Eq. 15 analytically for all the models.

The approaches employed in this work to evaluate the shear modulus are summarized in Tables 1 and 2, together with the pertinent expressions and parameter settings for Eq. 15. It is worth noting that the monomeric friction coefficient

**Table 1** Summary of Rouse relaxations employed in calculating the shear modulus. The core modulus function refers to the nomenclature of Eq. 11

| Model | Core modulus $m_{\text{Rouse}}$ | Second integral of Eq. 15 |
|---|---|---|
| UR | Eq. 1 | $M_i = 0, M_f = M_e$ |
| ER3 | Eq. 3 with $\kappa = 1/3$ | $M_i = 0, M_f \to \infty$ |
| ER5 | Eq. 3 with $\kappa = 1/5$ | $M_i = 0, M_f \to \infty$ |

**Table 2** Summary of reptation models employed in calculating the shear modulus. The core modulus function refers to the nomenclature of Eq. 11

| Model | Core modulus $m_{\text{single}}$ | First integral of Eq. 15 |
|---|---|---|
| DE | Eqs. 4 and 6 | $\beta$ tunable, $M_i = M_e, M_f \to \infty$ |
| DECLF | Eq. 7 | $\beta$ tunable, $M_i = M_e, M_f \to \infty$ |
| TDD | Eqs. 8 and 9 | $\beta$ tunable, $M_i = M_e, M_f \to \infty$ |
| MML[a] | Eqs. 12 and 13 | $\beta = 1, M_i = 10M_e, M_f \to \infty$ |

[a]It should recalled that $\beta$ is a dummy variable for this model, since the CR mechanisms are controlled by the $c_v$ parameter (Likhtman and McLeish 2002)

$\zeta_0$ and $G_N^0$ are the sole temperature-dependent parameters of all the models, with $\zeta_0$ much more temperature-dependent than $G_N^0$. In addition, in this work, the behavior of short chains was taken into account by an "inverse" isofrictional correction (Andreozzi et al. 2008) as detailed later in the manuscript.

## Materials and methods

In this work, we study ten PEA samples (Table 3), characterized by narrow molecular weight distributions and different molar masses (molar mass of PEA repeating unit $M_0 = 100$ g mol$^{-1}$). The polymer samples were synthesized following the atom transfer radical polymerization (Andreozzi et al. 2006). Number average $M_n$ and weight average $M_w$ molar masses were determined by size exclusion chromatography (SEC) using monodisperse polystyrene standards for column calibration (Andreozzi et al. 2006). For some samples, light scattering experiments were also carried out that confirmed mass measurements obtained with SEC. As in

**Table 3** Mass averages, polydispersity index and glass transition temperatures of PEA samples, ordered with decreasing magnitude of $M_n$

| Sample | $M_n$ (kg mol$^{-1}$) | $M_w$ (kg mol$^{-1}$) | $M_w/M_n$ | $T_g$ (K) |
|---|---|---|---|---|
| PEA20R | 120.00 | 150.00 | 1.25 | 253 |
| PEA06R | 58.20 | 66.50 | 1.15 | 253 |
| PEA05R | 24.90 | 26.60 | 1.07 | 253 |
| PEA04R | 18.65 | 20.20 | 1.08 | 250 |
| PEA02R | 11.65 | 13.10 | 1.13 | 252 |
| PEA18R | 8.80 | 9.60 | 1.09 | 250 |
| PEA01R | 7.50 | 8.25 | 1.10 | 248 |
| PEA17R | 7.30 | 7.80 | 1.07 | 247 |
| PEA16R | 2.75 | 3.00 | 1.09 | 243 |
| PEA15R | 0.98 | 1.20 | 1.22 | 231 |

Andreozzi et al. (2006), in this study the density $\rho$ of PEA samples is taken as 1.12 g cm$^{-3}$ (Wen 1999).

Differential calorimetry measurements were performed by means of a PerkinElmer DSC7 calorimeter to obtain the glass transition temperatures $T_g$ of the samples that were evaluated according to the onset definition (Hohne et al. 2003). Thermograms were recorded on heating at 10 K min$^{-1}$ after a quench at 40 K min$^{-1}$.

A Haake RheoStress RS150H stress-controlled rheometer was used, equipped with a RS150H Peltier system and a programmable thermal bath. A sensor with cone-plate geometry (35 mm diameter, cone angle 4°) was utilized for PEA15R sample, while a parallel plate system (diameter 20 mm) was chosen for the other samples. In rheological measurements at different temperatures, the thermal dilatation of the system was taken into account by varying the gap of the sensors, all the gaps being chosen to ensure gap independent measurements. A flux of ultrapure nitrogen gas was injected into the rheometer cell to avoid aqueous condense for measurements at temperatures lower than the ambient one.

All measurements were carried out in linear viscoelastic regime of the materials. Isothermal frequency sweeps were measured from $10^{-2}$ to 24.4 Hz. Zero shear viscosity was evaluated (Andreozzi et al. 2006) in independent ways from creep, creep recovery, and flow experiments at various temperatures and from the complex modulus in oscillatory measurements (Macosko 1994; Morrison 2001).

Viscosity and thermal parameters were discussed in a previous paper (Andreozzi et al. 2006). Recurring to time-temperature superposition principle (TTS) master curves (Hiemenz and Lodge 2007) were obtained by mathematical shifting of the isotherm frequency sweeps of the complex modulus $G^*(\omega)$ to the reference temperature $T_r = 270$ K, according to a literature procedure (Honerkamp and Weese 1993). The mass-independent value of the material parameter plateau modulus $G_N^0$ was previously obtained experimentally in high PEA polymers (Andreozzi et al. 2006), resulting in $G_N^0 = (2.1 \pm 0.1) \times 10^5$ Pa at 270 K; from that, it comes $M_e = 12$ kg mol$^{-1}$ evaluated following the "F" definition of Larson et al. (2003) and the minimum of tan$\delta$ criterion.

The master curve fitting was obtained via a C++ code. The experimental master curves were preliminarily interpolated sampling the frequency according to a geometric progression of ratio 2. $G'_{\exp}(\omega)$ and $G''_{\exp}(\omega)$ were thus obtained. Also, experimental data provided by GPC experiments were interpolated after sampling geometrically log$M$. The procedure provided $w(M)$ with at least 20 points per molar mass decade. To make a quantitative comparison between the experimental master curves and the theoretical ones $G^*_{\text{th}}(\omega)$ with $n$ fitting parameters, the reduced $\chi_r^2$ function

$$
\chi_r^2 = \frac{1}{P-n} \sum_{k=1}^{P} \left( \frac{\log \left( G'_{\exp}(\omega_k) / G'_{\text{th}}(\omega_k) \right)}{\sigma} \right)^2
$$
$$
+ \frac{1}{P-n} \sum_{k=1}^{P} \left( \frac{\log \left( G''_{\exp}(\omega_k) / G''_{\text{th}}(\omega_k) \right)}{\sigma} \right)^2 \quad (16)
$$

was then minimized by means of a Nelder–Mead routine (Nelder and Mead 1965) over $P$ points, implemented on purpose.

In the routine, a function is called to calculate $G^*_{\text{th}}(\omega)$. Such a function

1. Computes $m_{\text{single}}(t, M)$ and $m_{\text{Rouse}}(t, M)$ according to the dynamic models described in the theoretical section of this manuscript for each mass $M$ used in the sampling of $w(M)$. In the computation, it operates an "inverse" isofrictional correction (Andreozzi et al. 2008) in order to remove the intrinsic isofrictional behavior of the models and to adhere to the experimental data affected by different chain mobility (see Section "Results and discussion").

2. Uses the Eq. 15 to calculate $G^*_{\text{th}}(t)$ according to the guidelines detailed at the end of the previous section in order to account for molar mass distribution and possible CR mechanism.

3. Adopts different strategies to obtain the $G^*_{\text{th}}(\omega)$ function in the angular frequency domain: for Rouse relaxation the dynamic modulus was obtained analytically, Fourier-transforming the second term of Eq. 15; on the other hand, the complex modulus of reptation models was obtained by Schwarzl approximations (Schwarzl 1971), which were preferred over the numerical Fourier transform approach because of their simplicity and the associated computational speed.

A global maximum relative error of $\sigma = 7.0$ % was used in the minimization of Eq. 16, which is reliable enough in consideration of the experimental uncertainty and the master curve building.

## Results and discussion

### Relaxation of slightly entangled PEA chains

The master curves of dynamic moduli $G'$ and $G''$ of the samples PEA02R and PEA04R are shown in Fig. 1. According to the values of $M_w$ given in Table 3 and of the PEA entanglement mass $M_e$ evaluated in Andreozzi et al. (2006), these samples have $M_w$ greater than $M_e \approx 12$ kg mol$^{-1}$ and lower than $M_c \approx 2M_e$ (Andreozzi et al. 2006). Therefore, following the polymer dynamics theories, these samples should be
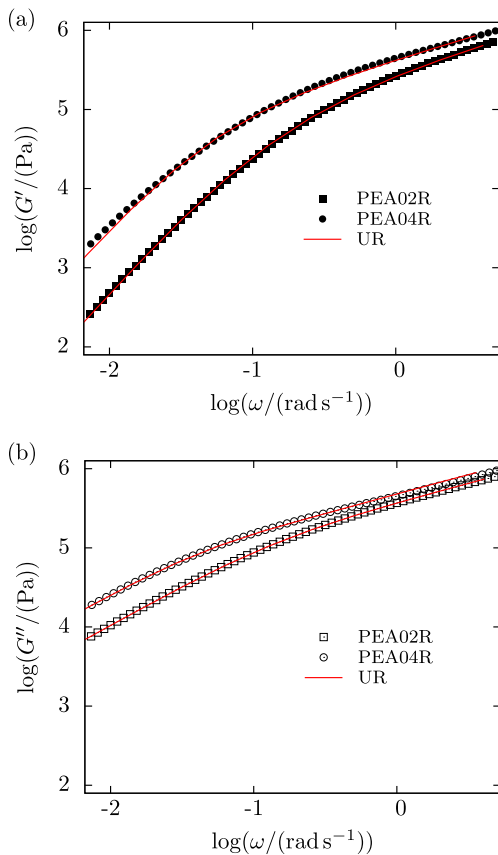
Fig. 1 Experimental master curves of $G^*$ for the slightly entangled PEA samples PEA02R and PEA04R. $G'$ (**a**) and $G''$ (**b**) moduli, calculated according to UR model, are superimposed to the experiment

subjected to entanglement. However, PEA02R and PEA04R do not show any plateau modulus in their master curves and, in addition, it was demonstrated (Andreozzi et al. 2006) that the isofrictional viscosity of these samples obeyed to a linear dependence on the molar mass, in accordance with the Rouse model.

To prove that the reptation is actually determinant for a proper description of the mechanical response of those PEA melts, we calculated master curves and compared the values of microscopic parameters both with Rouse model only (UR, Table 1) and with the combination of the different models of reptation, proposed in Table 2, with the Rouse modes for entangled melts (ER5, Table 1).

In all the calculations, we decided to adopt a correction for the monomeric friction coefficient $\zeta_0$. In fact, a rheological study, carried out according to the Rouse model for the unentangled PEA samples (PEA15R, PEA16R, PEA17R, PEA01R, and PEA18R), resulted in fits of very good quality, but provided a monomeric friction coefficient, set as a free parameter, with values strongly dependent on the polymer mass (Andreozzi et al. 2008). As an example, calculations for PEA17R and PEA18R samples provided $b^2\zeta_0 = (6.7 \pm 0.1) \times 10^{-24}$ N s m and $b^2\zeta_0 = (1.98 \pm$

$0.03) \times 10^{-23}$ N s m, respectively. This was ascribed to the different available free volume in the different melts.

Actually, all the dynamic models considered in this work assume isofrictional relaxation times, while, as well established in the literature (Andreozzi et al. 2006; Andreozzi et al. 2008; Colby et al. 1987), a highly mass-dependent $\zeta_0$ is found for polymer chains of low molar masses (Andreozzi et al. 2006; Andreozzi et al. 2008; Colby et al. 1987; Doi and Edwards 1988) because of the different mobility of the chains consequent upon the distinct concentration of chain ends (Colby et al. 1987). This experimental result leads to non-invariant $\zeta_0$ values for polymers with high and low molar masses and then to different values of $K_R$. Colby and coworkers proposed a scaling equation in Colby et al. (1987) in order to reduce the experiments to isofrictional results, coherent with theoretical models. In this paper, the reverse approach is needed. In fact, the experimental master curves result from the contribution of chains of different mass and distinct mobility, each of them with the pertinent $\zeta_0$. Then, because a single scaling factor does not work over all the components of the molar mass distribution, the assumption of mass-independent $\zeta_0$ was removed from the calculation of the theoretical master curve (Eq. 15) by applying a scaling, reciprocal of the one of Colby et al. (1987).

More precisely, the following correction of the monomeric friction coefficient is necessary to tune up the theoretical master curves with the experiments (Andreozzi et al. 2008):

$$\zeta_0(M)/\zeta_0 = 10^{c_{1\infty}-c_1(M)} \tag{17}$$

where $c_1(M)$ is the Williams–Landel–Ferry (WLF) parameter $c_1$ (Ferry 1980) at the molar mass $M$; $c_{1\infty}$ is the WLF parameter at very high molar masses (in the limit $M \to \infty$). The rescaling of Eq. 17 provides an "inverse" correction with respect to the one found in the literature (Andreozzi et al. 2006; Colby et al. 1987), which is adopted when experimental data of viscosity are requested to fit the theoretical behavior.

It is worth noting that, according to free-volume theories (Andreozzi et al. 2006; Pearson et al. 1994; Richter et al. 1994), the function $c_1(M)$ can be expressed analytically as (Andreozzi et al. 2006; Andreozzi et al. 2008)

$$c_1(M) = c_{1\infty} \frac{M}{M + M_{c_1}} \tag{18}$$

The parameters $c_{1\infty}$ and $M_{c_1}$ for PEAs were determined in Andreozzi et al. (2006) from WLF parameters obtained by the master curve construction at the reference temperature $T_r = 270$ K and resulted to be $c_{1\infty} = 9.12$ and $M_{c_1} = 0.58$ kg mol$^{-1}$.

In Fig. 1, the master curves of PEA02R and PEA04R calculated according to the UR model are shown. The high

**Table 4** UR fitting parameters for slightly entangled (PEA02R and PEA04R) and unentangled PEA melts, listed with decreasing $M_n$

| Sample | $K_R$ (ms) | $\chi_r^2$ |
|--------|-----------|-----------|
| PEA04R | 1.07 | 1.4 |
| PEA02R | 0.85 | 0.8 |
| PEA18R | 0.79 | 1.8 |
| PEA01R | 0.80 | 1.0 |
| PEA17R | 0.76 | 0.6 |
| PEA16R | 0.81 | 0.8 |
| PEA15R | 0.76 | 0.6 |

quality of the fits can be appreciated, also from the pertinent $\chi_r^2$ reported in Table 4. Table 4 also lists the $K_R$ values (see Eq. 2). The results do not match the model, even with the correction of Eq. 17, and provide a clear indication that reptation plays a role in this molar mass range. For comparison purposes, Table 4 also reports the values pertinent to the unentangled samples (Andreozzi et al. 2008). For them, the iso-free-volume correction of Eq. 17 was effective and provided coherent $K_R$ values, resulting in a mean $b^2 \zeta_0 = (7.8 \pm 0.2) \times 10^{-23}$ N s m (Andreozzi et al. 2008). It is seen (Table 4) that the $K_R$ value of PEA02R and PEA04R is beyond the 95 % confidence interval (Martinelli and Baldini 2008; Taylor 1997).

Then, we calculated the dynamic moduli of PEA02R and PEA04R with different reptation models, either including or not CR relaxation, and letting $M_e$, $K_R$, and one reptation parameter (see Table 5) to be free parameters. One expects that the best fitting of the master curves provides free-parameter values independent of the sample (e.g., $M_e$ constant over the whole set of PEA samples) and dependent on the model only. Also, the applicability or not of the model is determined by the fluctuation amount of the free parameters.

It must be noted that, at this stage, all the calculations were carried out setting at 3 the number of free parameters of each model and constraining the others to preset values. In particular, $\beta$ (Eq. 15), for all the models, and $c_v$ for MML were always constrained as shown in Table 5. Regarding $K_d$, its values were calculated, for models other than DE, during the fitting procedure according to the Eqs. 5 and 6 with $\alpha = 3$. In the DE model case, $K_d$ was set as free and $\alpha$ (Eq. 6) was constrained to the literature value of 3.4.

In Fig. 2, experimental master curves of PEA02R and PEA04R are compared with $G'$ and $G''$ calculated by combining ER5 and, from time to time, DE, DECLF, TDD, and MML reptation models, in the absence of the CR relaxation. In Fig. 3, the experimental master curves are compared to the calculated ones, by using the same models, each of them including the CR mechanism.

**Table 5** Parameters for slightly entangled PEA02R and PEA04R from 3 free-parameter fitting procedures according to reptation models

| Sample | Model | CR[a] | $M_e$ (kg mol$^{-1}$) | $K_R$ (ms) | $K_d/K_R$ | Reptation par. | $\chi_r^2$ |
|--------|-------|-------|----------------------|-----------|-----------|----------------|-----------|
| PEA02R | DE | No, $\beta = 1$ | Undetectable[b] | 0.85 | Undetectable[b] | $\alpha = 3.4$[a] | 0.7 |
| | DECLF | No, $\beta = 1$ | 29.0 | 0.83 | Derived[d] | $v = 0.4$ | 0.6 |
| | TDD | No, $\beta = 1$ | 20.0 | 0.81 | Derived[d] | $M_d = 350$ kg mol$^{-1}$ | 0.6 |
| | MML | No, $c_v = 0$[c] | Undetectable[b] | 0.85 | Derived[d] | $b$, undetectable[e] | 0.7 |
| | DE | Yes, $\beta = 2.1$ | 14.5 | 0.79 | 330 | $\alpha = 3.4$[a] | 0.6 |
| | DECLF | Yes, $\beta = 2.1$ | 11.7 | 0.77 | Derived[d] | $v = 0.1$ | 0.6 |
| | TDD | Yes, $\beta = 2.1$ | 12.1 | 0.78 | Derived[d] | $M_d = 21$ kg mol$^{-1}$ | 0.6 |
| | MML | Yes, $c_v = 1$[c] | 14.5 | 0.79 | Derived[d] | $b = 6$ Å | 0.6 |
| PEA04R | DE | No, $\beta = 1$ | 17.0 | 0.76 | 115 | $\alpha = 3.4$[a] | 2.2 |
| | DECLF | No, $\beta = 1$ | 9.5 | 1.18 | Derived[d] | $v = 2.2$ | 3.8 |
| | TDD | No, $\beta = 1$ | 8.5 | 1.23 | Derived[d] | $M_d = 2000$ kg mol$^{-1}$ | 4.0 |
| | MML | No, $c_v = 0$[c] | 28.5 | 1.03 | Derived[d] | $b$, undetectable[e] | 1.6 |
| | DE | Yes, $\beta = 2.1$ | 14.4 | 0.79 | 370 | $\alpha = 3.4$[a] | 1.1 |
| | DECLF | Yes, $\beta = 2.1$ | 12.5 | 0.80 | Derived[d] | $v = 0.1$ | 0.6 |
| | TDD | Yes, $\beta = 2.1$ | 11.7 | 0.79 | Derived[d] | $M_d = 30$ kg mol$^{-1}$ | 0.8 |
| | MML | Yes, $c_v = 1$[c] | 17.5 | 0.89 | Derived[d] | $b = 5$ Å | 1.4 |

[a] Constrained values

[b] Undetectable: the fitting procedure determines an $M_e$ higher than the highest mass content of the molar mass distribution. This means that practically the UR fit was obtained

[c] In this case, $\beta$ of Eq. 15 is a dummy variable, to be set to 1

[d] Calculated during the fitting procedure according to Eqs. 5 and 6, using the running values of the $M_e$ and $K_R$ free parameters

[e] Note that in the absence of CR, the MML model reduces to 2 the number of free parameters being $b$ only accounted for in the CR function $R(c_v, t)$
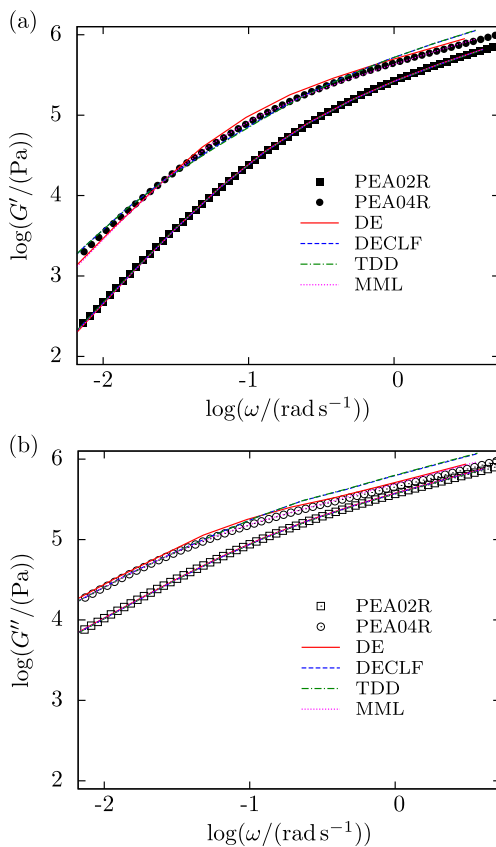
**Fig. 2** Slightly entangled PEAs: 3 free-parameter reptation models without CR. Experimental master curves and superimposed calculated $G'$ (**a**) and $G''$ (**b**) moduli are shown for PEA02R and PEA04R, respectively



**Fig. 3** Slightly entangled PEAs: 3 free-parameter reptation models with CR. Experimental master curves and superimposed calculated $G'$ (**a**) and $G''$ (**b**) moduli are shown for PEA02R and PEA04R, respectively

In both the cases, the fitting parameters are summarized in Table 5. Once applied to PEA02R and PEA04R, all these models provided master curves of good quality, with values of $\chi_r^2$ within the 95 % confidence interval (Martinelli and Baldini 2008; Taylor 1997), excluding the case of DE, DECLF, and TDD without CR for the PEA04R sample.

An analysis of the fitting parameters could provide more insight and a discrimination guide to select the dynamic model more appropriate to the slightly entangled PEA polymers.

At first, we start with inspecting reptation without CR relaxation. The $K_R$ value obtained with reptation models without CR is in accordance with its mean value retrieved with UR model in unentangled PEA samples (Table 4) only for DE model in PEA04R. Moreover, when applied to this latter sample, DE, DECLF, and TDD models show rejectable values for $\chi_r^2$. Simultaneously, for all these models without CR relaxation, it is observed that the $M_e$ value, if evaluated by the fit, turns out to be either greater or smaller than the one evaluated according
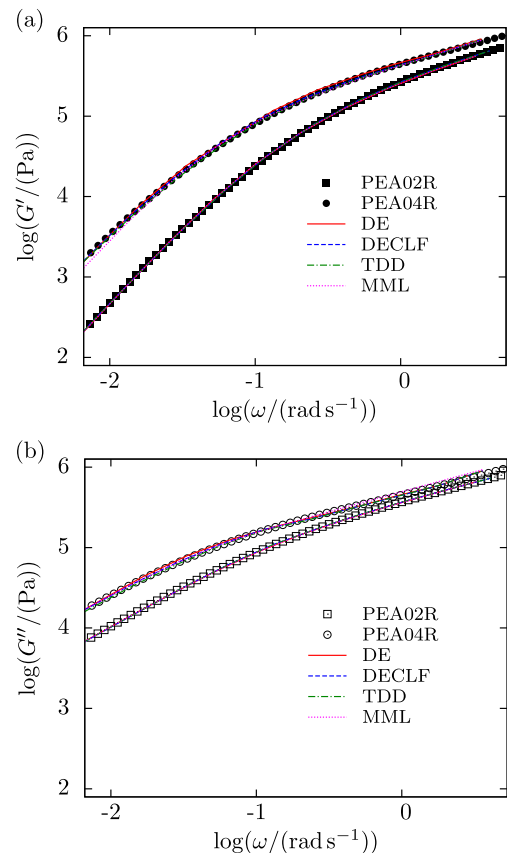
to the entanglement plateau of PEAs in Andreozzi et al. (2006). This finding leads to an evident disagreement with respect to the well-established result $M_c/M_e \approx 2$ (Doi and Edwards 1988), being $M_c$ about 26 kg mol$^{-1}$ in PEAs (Andreozzi et al. 2006). In particular, MML model foresees for PEA04R a very high value of $M_e$. On the other hand, for PEA02R, no plausible $M_e$ value was provided by simulations according to DE and MML models. Indeed, the estimated $M_e$ fell at so high values that the reptation dynamics could have taken place for masses overrunning on the available mass distribution of the sample.

Regarding $K_d$, a free parameter in DE model case, unphysical variations were found for PEA04R, with values by far less than the values of $K_d = 620 K_R$ that could be retrieved from calculations carried out according to Eq. 5, Eq. 6, and the $K_R$ values, as resulting from the fitting procedures. On the other hand, for PEA02R, the fitting procedure was not able to provide any result different from the outcome that was formerly obtained by using the UR model. The collection of all these considerations allowed us to rule
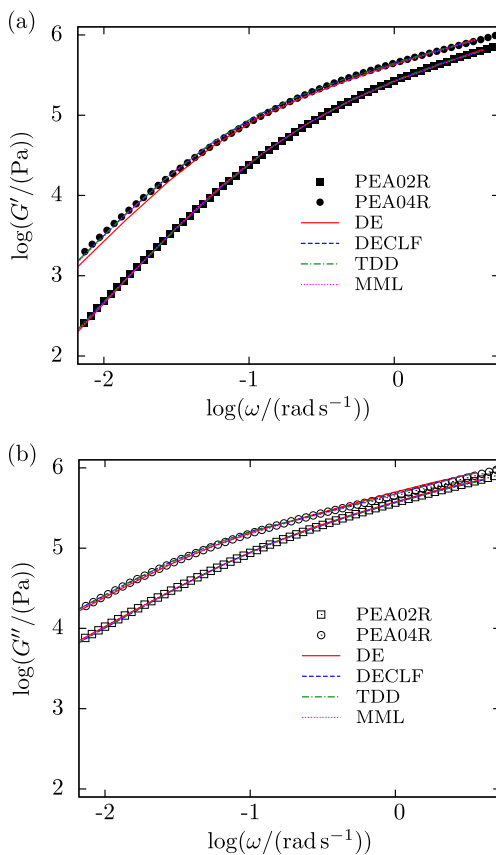
**Fig. 4** Slightly entangled PEAs: 4 free-parameter reptation models with CR. Experimental master curves and superimposed calculated $G'$ (**a**) and $G''$ (**b**) moduli are shown for PEA02R and PEA04R, respectively



**Fig. 5** Slightly entangled PEAs: 4 free-parameter reptation models without CR. Experimental master curves and superimposed calculated $G'$ (**a**) and $G''$ (**b**) moduli are shown for PEA02R and PEA04R, respectively

out all reptation models that not included CR mechanism.

The best fit parameters from reptation models including CR mechanism are also available in Table 5. Inspecting $\chi_r^2$, a remarkable global enhancement of the fit quality is now obtained for PEA04R, for which the molar mass is higher than for PEA02R and probably the reptation contribution to its dynamic moduli becomes dominant.

A glance at the results for $K_R$ and $M_e$ shows that their value is much more homogeneous over the whole model and sample set and generally comparable to both the $K_R$ value of unentangled PEA series and the $M_e$ value obtained from the entanglement plateau evaluation: actually, the values of $M_e$ (Table 5), in presence of CR, stabilize at about $12-16$ kg mol$^{-1}$. This indicates that the CR mechanism is important in describing the dynamics of these slightly entangled PEA polymers. Moreover, recalling the unphysical $K_R$ results from application of the UR model to PEA02R and PEA04R (Table 4), it seems possible to conclude that the change in the outcome of $K_R$, and then of the monomeric friction coefficient, signals the onset of entanglement in passing from the unentangled PEA series studied in Andreozzi et al. (2008) to PEA02R and PEA04R samples.
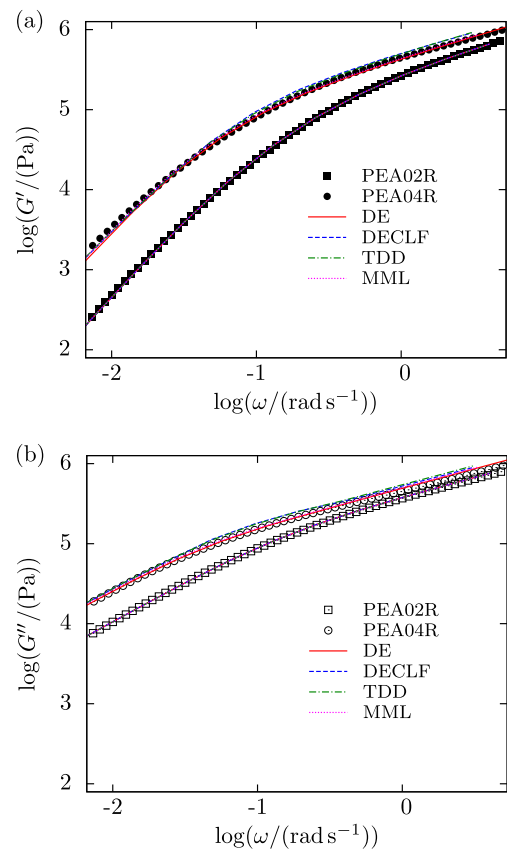
To get more insight, a more refined analysis of the parameters allows a selection among the models. It appears that the DE model should be abandoned, even after including CR. In fact, while the quality of the fit is good, the values obtained for $M_e$ are indeed quite different, in comparison with the consistence exhibited by the results from the DECLF and TDD models. Moreover, the $K_d$ free parameter of DE admittedly shows very similar values for the slightly entangled PEAs (Table 5), but the empirical nature of Eq. 6 in the DE model makes difficult to obtain quantitative information about the terminal region of the master curves. To summarize, the DE model provides good quality fits and a very fast and simple calculation of slightly entangled master curves, but the obtained parameters allow only a rough estimation of $M_e$, and it is not possible to quantitatively link the disengagement and the Rouse time.

On the other hand, looking at DECLF and TDD implemented with CR relaxation mechanism, they appear to provide not only $K_R$ in accordance with the unentangled PEA series, but also $M_e$ nicely close to 12 kg mol$^{-1}$ and in agreement with the evaluation of the entanglement mass from

the entanglement plateau of PEAs (Andreozzi et al. 2006). Moreover, the linking between disengagement and Rouse times via Eq. 5 makes these models promising also for quantitative considerations on the monomeric friction coefficient. However, at this stage, it should be noted that the values of the reptation parameter $M_d$, obtained from TDD with CR in PEA02R and PEA04R, are not constant and are small with respect to the literature results (van Ruymbeke et al. 2002) for entangled polystyrene (PS), which is a polymer exhibiting similar $M_e$ values. The finding here could be ascribed to the low molar mass of the specific nearly entangled PEA samples, being TDD model known to be unable to correctly predict relaxation of short chains (van Ruymbeke et al. 2002).

Regarding the MML model with $c_v = 1$, the parameters show intriguing features such as the effectiveness of the correlation between disengagement and Rouse times via Eq. 5, and the values of $M_e$ with the right order of magnitude, but greater than 12 kg mol$^{-1}$. Nonetheless, the MML model applied to PEA04R provides the highest $\chi_r^2$ among the models with CR, and a value of $K_R$ quite different from the expected one. At a first glance, these last issues could be ascribed to the $c_v$ value, constrained to 1, or to the upper limit of the summations in Eqs. 13a and 13d set to $(Z/10)^{1/2}$ as in Likhtman and McLeish (2002). A deeper analysis showed that the MML model is not that sensitive

to these choices, as also stated in Likhtman and McLeish (2002). Therefore, the obtained $K_R$ values could come from the definition of $\tilde{\tau}_f$ (Eq. 13b), which could be not suitable for PEAs.

Up to now, the results show that some reptation models with a 3 parameter fitting provide in nearly entangled PEAs microscopic quantities consistent with the oligomer series.

In some literature studies, the disengagement time $K_d$, which is a mass-independent coefficient, is set as a free parameter (van Ruymbeke et al. 2002). For comparison purposes and with the aim to eventually clarify some of the above topics and flaws, the calculations of the complex modulus $G^*$ were extended in this work to the case of 4 free fitting parameters. As an additional intent, evidence is expected to be obtained regarding the validity of the results from 3 parameter fitting procedure: quality of the fits and values of the parameters should be quite unchanged despite the additional free fitting parameter. Any constraint over the $K_d$ value was then removed in simulations of slightly entangled PEAs for DELCF, TDD, and MML models and the value of the parameter $\alpha$ for DE model was also set as free. In Figs. 4 and 5, the experimental master curves are compared to the calculated ones, by using the 4 free-parameter models, including or not CR, respectively. Fitting parameters are summarized in Table 6.

**Table 6** Parameters for slightly entangled PEA02R and PEA04R from 4 free-parameter fitting procedures according to reptation models

| Sample | Model | CR[a] | $M_e$ (kg mol$^{-1}$) | $K_R$ (ms) | $K_d/K_R$ | Reptation par. | $\chi_r^2$ |
|---|---|---|---|---|---|---|---|
| PEA02R | DE | No, $\beta = 1$ | Undetectable[b] | 0.85 | Undetectable[b] | $\alpha$, undetectable[b] | 0.8 |
| | DECLF | No, $\beta = 1$ | Undetectable[b] | 0.85 | Undetectable[b] | $v$, undetectable[b] | 0.8 |
| | TDD | No, $\beta = 1$ | Undetectable[b] | 0.85 | Undetectable[b] | $M_d$, undetectable[b] | 0.8 |
| | MML | No, $c_v = 0$[c] | Undetectable[b] | 0.85 | Undetectable[b] | $b$, undetectable[d] | 0.8 |
| | DE | Yes, $\beta = 2.1$ | Undetectable[b] | 0.84 | Undetectable[b] | $\alpha$, undetectable[b] | 0.6 |
| | DECLF | Yes, $\beta = 2.1$ | 10.4 | 0.72 | 50,500 | $v = 0.3$ | 0.6 |
| | TDD | Yes, $\beta = 2.1$ | 10.8 | 0.76 | 38,000 | $M_d = 26$ kg mol$^{-1}$ | 0.6 |
| | MML | Yes, $c_v = 1$[c] | 15.8 | 0.80 | 43,000 | $b = 3$ Å | 0.6 |
| PEA04R | DE | No, $\beta = 1$ | 14.5 | 1.05 | 55 | $\alpha = 1.6$ | 1.2 |
| | DECLF | No, $\beta = 1$ | 12.8 | 0.79 | 7300 | $v = 0.1$ | 1.4 |
| | TDD | No, $\beta = 1$ | 13.8 | 0.87 | 26,500 | $M_d = 245$ kg mol$^{-1}$ | 1.4 |
| | MML | No, $c_v = 0$[c] | 20.5 | 1.04 | 22 | $b$, undetectable[d] | 1.0 |
| | DE | Yes, $\beta = 2.1$ | 14.5 | 0.79 | 350 | $\alpha = 3.4$ | 1.1 |
| | DECLF | Yes, $\beta = 2.1$ | 13.5 | 0.80 | 84,000 | $v = 0.25$ | 0.6 |
| | TDD | Yes, $\beta = 2.1$ | 14.0 | 0.81 | 49,000 | $M_d = 17$ kg mol$^{-1}$ | 0.6 |
| | MML | Yes, $c_v = 1$[c] | 16.0 | 0.89 | 64,000 | $b = 7$ Å | 0.8 |

[a]Constrained values

[b]Undetectable: the fitting procedure determines a parameter value corresponding to an unentangled polymer. This means that practically the UR fit was obtained

[c]In this case, $\beta$ of Eq. 15 is a dummy variable, to be set to 1

[d]Note that in the absence of CR, the MML model reduces to 3 the number of free parameters being $b$ only accounted for in the CR function $R(c_v, t)$

Inspection of Figs. 4 and 5 and Table 6 shows that, in general, an additional free parameter hardly improves the curves and the parameter values calculated according to DE, DECLF, TDD, and MML models. This finding is confirmed by the $\chi_r^2$ values that are practically unchanged in most cases and are now fixed for the PEA04R simulations with TDD and DECLF models without CR.

Indeed, it is seen that the values of the parameters from calculations including CR mechanism (Table 6) are only slightly changed with respect to the ones pertaining to the 3 free-parameter simulations (Table 5). The sole different result pertains to the DE model applied on PEA02R, whose outcome would locate the sample outside the entanglement region. This conclusion parallels the one provided after applying to PEA02R the DE model without CR and with 3 free fitting parameters. Furthermore, $\chi_r^2$ is practically unchanged for the DE, DECLF, and TDD models in both the samples. Then, one can conclude that for these models there is no need of adding a further degree of freedom to improve the goodness of the fit. On the other hand, in the case of the MML model, unlocking $K_d$ allows a significant improvement of the quality of the fit for PEA04R, but gives fluctuating values for the $b$ reptation parameter. This confirms that assumptions about relaxation times or upper limits set in the MML model by Eq. 13 are not effective in finely determining the dynamics of slightly entangled samples.

As a matter of fact, an appreciable improvement in fit quality can be found instead after increasing to 4 the number of free parameters when CR mechanism was omitted. However, the additional free parameter did not allow the recovery of physical meaning for those parameters that, in the 3 free-parameter calculations, were not consistent with the assumptions of the theory (e.g., mass-independent values for $M_e$ and $K_R$, relationship of $K_R$ and $K_d$ through Eqs. 5 and 6 with $\alpha = 3$). Furthermore, introducing a fourth parameter causes a general loss of significance for those parameters of PEA02R that in Table 5 still had some consistence with other (literature) experimental findings.

To summarize the results of the present section, the sample-by-sample fitting procedure of the slightly entangled PEA samples, implemented with the isofrictional correction, has shown that the analysis of the coherence of the free parameters is a powerful tool that allows to harmonize material parameters each other and with the data pertinent to low molecular weight PEAs. Moreover, it provides reptation models with CR relaxation mechanism as eligible models for describing the dynamics of these samples. In particular, 4 free-parameter calculations have shown not to compensate the 3 free-parameter calculations with CR, evidencing the need of including this relaxation mechanism also at this mass values.
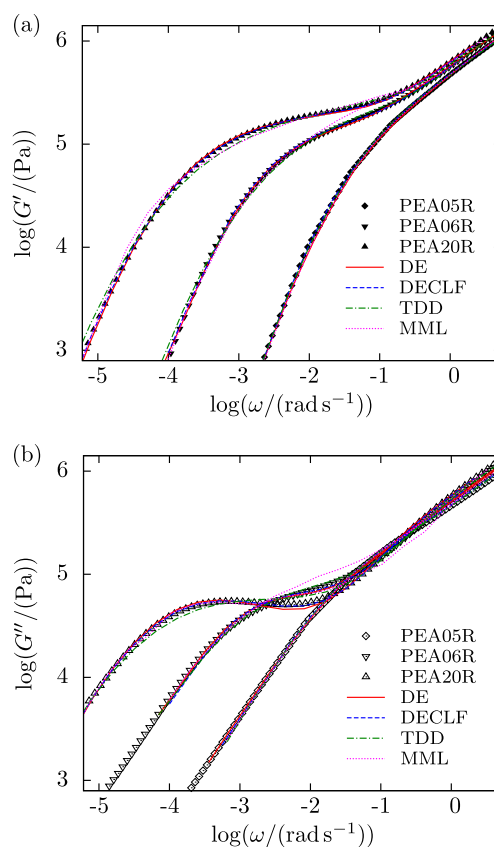


**Fig. 6** Entangled PEA05R, PEA06R, and PEA20R samples: 3 free-parameter reptation models with CR. Experimental master curves and superimposed calculated $G'$ (**a**) and $G''$ (**b**) moduli

## Relaxation of well-entangled PEA samples

In the previous section, we have shown that reptation models become effective for molar masses at $M_e$, namely 12 kg mol$^{-1}$ for PEA. The molar masses of PEA05R, PEA06R, and PEA20R samples rank well above this value and their $G^*$ master curves show entanglement plateau (e.g., Fig. 6). Because of these features, these samples offer an effective test for reptation models. Satisfactory reptation models are expected to provide values of the parameters consistent with the ones found in the previous section. In particular, we expect coherent values of the entanglement mass $M_e$ and of $K_R$ over the whole range of PEA molar masses. Incidentally, it must be noted that the high molar mass of these well-entangled samples makes ineffective the isofrictional correction of Eq. 17. Being well-entangled polymers usually employed to verify reptation theories, this justifies the lack of studies in the literature that take into account the "inverse" isofrictional correction.

In Fig. 6, experimental master curves of PEA05R, PEA06R, and PEA20R are compared with $G^*$ curves calculated by combining ER5 and, from time to time, DE, DECLF, TDD, and MML reptation models (with 3 free
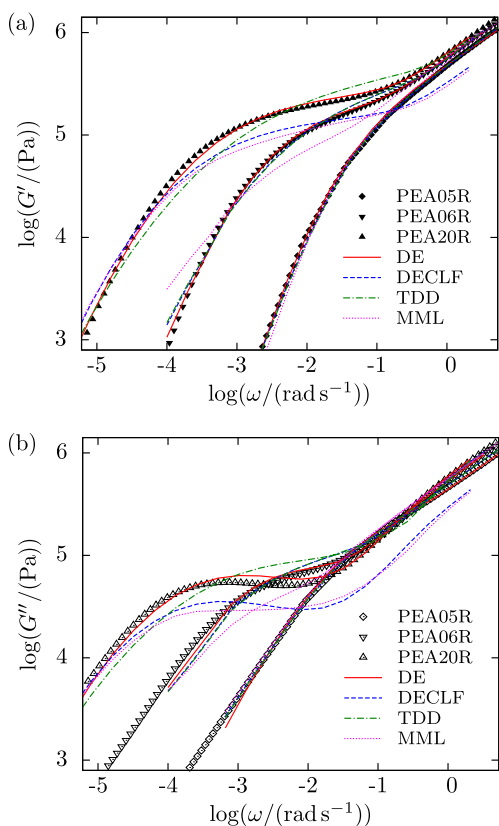
**Fig. 7** Entangled PEA05R, PEA06R, and PEA20R samples: 3 free-parameter reptation models without CR. Experimental master curves and superimposed calculated $G'$ (**a**) and $G''$ (**b**) moduli

parameters), each of them including CR. In Fig. 7, experimental master curves are compared with the calculated ones, by using the same models in the absence of CR relaxation. Fitting parameters are summarized in Table 7.

It is apparent that from inspection of Figs. 6 and 7 and the pertinent $\chi_r^2$ reported in Table 7, the good fits are obtained in the presence of CR relaxation and poor quality is retrieved with reptation models without CR relaxation. Moreover, without CR, the higher the molar mass of the sample, the worse the fits and the $\chi_r^2$ values. Further confirmation is given by the values of the parameters of Table 7, signaling that the DECLF, TDD, and MML reptation models without CR mechanism fail also because of the values of $M_e$ and $K_R$, by far different from their expected values. Likewise, DE model without CR should be immediately discharged as a consequence that the values of $K_d$ differ orders of magnitude with respect to the molar-mass-independent values of $K_d$ retrieved from $K_R$ and Eqs. 5 and 6 with $\alpha = 3$. Therefore, CR mechanism is definitely demonstrated as a necessary ingredient to obtain fitting parameters with values both consistent each other and in accordance with the model.

After including CR, the DE model improves its performance, but still suffers from the intrinsic impossibility of

defining a reliable microscopic expression for $K_d$ when the power law $M^{3.4}$ is assumed. DECLF and TDD models, on the other hand, provide $K_R$ in accordance with the unentangled PEA series. Regarding $M_e$, in general, it appears nicely close to 12 kg mol$^{-1}$ and in agreement with its evaluation from the entanglement plateau of PEAs (Andreozzi et al. 2006), but its value fluctuates for the various samples in the TDD model. Also, it turns out that the parameter $v$ in DECLF is stable, having therefore smaller deviations with respect to its mean value across all the series with respect to the ones of $M_d$ reptation parameter of TDD. This definitely makes eligible DECLF with respect to the TDD model.

A particular mention has to be devoted to the $M_d$ values in the TDD model, which result to increase with the molar mass, up to a value about one order of magnitude greater than the $M_e$ mass. This finding is in agreement with the literature results on PS (van Ruymbeke et al. 2002)[2]. As previously noted, $M_e$ of PS was found to be of the same order of magnitude of the PEA one, and an evaluation of $M_d$, applying TDD on PS well-entangled samples, provided $M_d$ values one order of magnitude greater than the pertinent $M_e$ (Fetters et al. 1994; van Ruymbeke et al. 2002).

Regarding the MML model, $M_e$, $K_R$, and $b$ parameters for PEA06R and PEA20R, shown in Table 7, are consistent each other. $M_e$ and $b$ outcomes are quite in agreement with the forecasts, so that the reptation dynamics seems to be correctly taken into account. Nonetheless, $K_R$ is very different from the expected one. From these results, one can conclude that, to reproduce the experiments (in which the reptation is dominant), the MML model is compelled to track $\tilde{\tau}_f$ (Eq. 13b), with a consequent penalization of the Rouse relaxations.

For comparison purposes, the calculations of the complex modulus $G^*$ of entangled samples were extended to the case of 4 free fitting parameters. As in the case of nearly entangled PEAs, any constraint was removed over the $K_d$ value and, for the DE model, over the value of the parameter $\alpha$. In Table 8, the best-fit parameters are reported after including or not the CR relaxation in the main models. The best fits are compared with the experimental curves in Figs. 8 and 9, respectively.

Looking at the figures, it appears that 4 free-parameter models without CR mechanism sensibly improve the ability to reproduce the experiments with respect to the 3 free-parameter models without CR. However, the obtained fits are not satisfactory and the gauge is provided by the analysis of the parameters of the table, where it is seen

---

[2]In van Ruymbeke et al. (2002), the number of free fitting parameters was 3 as well, but $M_e$ was a fixed parameter, while $K_d$, $K_R$, and $M_d$ were left free.

**Table 7** Parameters for entangled PEA05R, PEA06R, and PEA20R from 3 free-parameter fitting procedures according to reptation models

| Sample | Model | CR[a] | $M_e$ (kg mol$^{-1}$) | $K_R$ (ms) | $K_d/K_R$ | Reptation par. | $\chi_r^2$ |
|---|---|---|---|---|---|---|---|
| PEA05R | DE | No, $\beta = 1$ | 13.0 | 0.79 | 70 | $\alpha = 3.4$[a] | 2.6 |
| | DECLF | No, $\beta = 1$ | 25.0 | 0.88 | Derived[b] | $v = 0.4$ | 0.6 |
| | TDD | No, $\beta = 1$ | 23.0 | 0.86 | Derived[b] | $M_d = 180$ kg mol$^{-1}$ | 0.8 |
| | MML | No, $c_v = 0$[c] | 15.5 | 0.99 | Derived[b] | $b$, undetectable[d] | 2.6 |
| | DE | Yes, $\beta = 2.1$ | 14.5 | 0.75 | 360 | $\alpha = 3.4$[a] | 0.8 |
| | DECLF | Yes, $\beta = 2.1$ | 12.8 | 0.78 | Derived[b] | $v = 0.1$ | 0.6 |
| | TDD | Yes, $\beta = 2.1$ | 14.6 | 0.76 | Derived[b] | $M_d = 21$ kg mol$^{-1}$ | 0.8 |
| | MML | Yes, $c_v = 1$[c] | 13.5 | 0.86 | Derived[b] | $b = 6.5$ Å | 0.6 |
| PEA06R | DE | No, $\beta = 1$ | 11.6 | 0.78 | 25 | $\alpha = 3.4$[a] | 1.2 |
| | DECLF | No, $\beta = 1$ | 6.0 | 0.91 | Derived[b] | $v = 4.3$ | 2.6 |
| | TDD | No, $\beta = 1$ | 6.0 | 0.90 | Derived[b] | $M_d = 4200$ kg mol$^{-1}$ | 3.0 |
| | MML | No, $c_v = 0$[c] | 15.2 | 0.85 | Derived[b] | $b$, undetectable[d] | 12.0 |
| | DE | Yes, $\beta = 2.1$ | 15.2 | 0.79 | 330 | $\alpha = 3.4$[a] | 0.9 |
| | DECLF | Yes, $\beta = 2.1$ | 12.0 | 0.80 | Derived[b] | $v = 0.1$ | 0.8 |
| | TDD | Yes, $\beta = 2.1$ | 8.0 | 0.81 | Derived[b] | $M_d = 200$ kg mol$^{-1}$ | 1.0 |
| | MML | Yes, $c_v = 1$[c] | 10.2 | 0.32 | Derived[b] | $b = 6.0$ Å | 1.4 |
| PEA20R | DE | No, $\beta = 1$ | 12.0 | 0.81 | 50 | $\alpha = 3.4$[a] | 1.6 |
| | DECLF | No, $\beta = 1$ | 16.4 | 0.20 | Derived[b] | $v = 0.01$ | 18.8 |
| | TDD | No, $\beta = 1$ | 6.0 | 0.82 | Derived[b] | $M_d = 18{,}900$ kg mol$^{-1}$ | 6.6 |
| | MML | No, $c_v = 0$[c] | 13.8 | 0.19 | Derived[b] | $b$, undetectable[d] | 18.0 |
| | DE | Yes, $\beta = 2.1$ | 15.0 | 0.78 | 300 | $\alpha = 3.4$[a] | 1.1 |
| | DECLF | Yes, $\beta = 2.1$ | 12.2 | 0.76 | Derived[b] | $v = 0.1$ | 0.9 |
| | TDD | Yes, $\beta = 2.1$ | 9.0 | 0.74 | Derived[b] | $M_d = 230$ kg mol$^{-1}$ | 1.5 |
| | MML | Yes, $c_v = 1$[c] | 10.0 | 0.33 | Derived[b] | $b = 5.0$ Å | 1.6 |

[a]Constrained values

[b]Calculated during the fitting procedure according to Eqs. 5 and 6, using the running values of the $M_e$ and $K_R$ free parameters

[c]In this case, $\beta$ of Eq. 15 is a dummy variable, to be set to 1

[d]Note that in the absence of CR, the MML model reduces to 2 the number of free parameters being $b$ only accounted for in the CR function $R(c_v, t)$

that unphysical results are obtained, for each model and sample, in correspondence of some mass invariant parameters. As in the case of the slightly entangled samples discussed in the previous section, this result is not unexpected because the additional free parameter is not effective in reproducing the relaxation details connected with the CR mechanism.

After introducing CR, still important fluctuations are associated to the values of mass-independent parameters, $K_R$, $M_e$, $K_d$, and $\alpha$, in some cases by far different from the expected values. We can then conclude that addition of a further free parameter does not improve sensibly the quality of the fits with CR mechanism, while it may lead to variations of the parameters incoherent with the theoretical models. Thus, 4 fitting parameters should be profitably discharged, being 3 parameter simulations able to discriminate among models and to suitably describe the PEA relaxation dynamics.

As a final result of our 4 fitting parameter study, we test the goodness of the hypothesis implied by the previous assumptions for $\beta$ and $c_v$. Figure 10 presents the result of best fitting at 4 free parameters of well-entangled PEA20R sample. The calculation was accomplished according to DECLF and MML models with $\beta$ and $c_v$, respectively, used as a free parameter together with $K_R$ and $M_e$, as well as the pertinent reptation parameter of the model.

From Fig. 10, it is seen that good fits are obtained, even if DECLF model appears more effective. This is signaled also by the values of the reduced chi-square of the fits $\chi_r^2 = 0.9$ for DECLF and $\chi_r^2 = 1.5$ for MML model. The other free parameters that were obtained resulted in $\beta = 2.11$, $M_e = 11.0$ kg mol$^{-1}$, $K_R = 0.78$ ms, $v = 0.25$ in the DECLF case, and $c_v = 0.8$, $M_e = 10.0$ kg mol$^{-1}$, $K_R = 0.34$ ms, $b = 5$ Å in the MML case. Comparing these values with the ones in Table 8, it is possible to conclude that, in both cases,

**Table 8** Parameters for entangled PEA05R, PEA06R, and PEA20R from 4 free-parameter fitting procedures according to reptation models

| Sample | Model | CR[a] | $M_e$ (kg mol$^{-1}$) | $K_R$ (ms) | $K_d/K_R$ | Reptation par. | $\chi_r^2$ |
|--------|-------|-------|------------------------|-------------|-----------|----------------|------------|
| PEA05R | DE | No, $\beta = 1$ | 21.4 | 1.27 | 4 | $\alpha = 2.8$ | 3.2 |
| | DECLF | No, $\beta = 1$ | 10.0 | 0.81 | 3500 | $v = 0.2$ | 3.0 |
| | TDD | No, $\beta = 1$ | 10.9 | 0.85 | 3000 | $M_d = 6$ kg mol$^{-1}$ | 2.6 |
| | MML | No, $c_v = 0^b$ | 16.0 | 0.97 | 99,000 | $b$, undetectable[c] | 1.4 |
| | DE | Yes, $\beta = 2.1$ | 31.3 | 1.06 | 3200 | $\alpha = 3.5$ | 1.2 |
| | DECLF | Yes, $\beta = 2.1$ | 14.2 | 0.79 | 81,600 | $v = 0.2$ | 0.6 |
| | TDD | Yes, $\beta = 2.1$ | 14.1 | 0.78 | 42,000 | $M_d = 12$ kg mol$^{-1}$ | 0.6 |
| | MML | Yes, $c_v = 1^b$ | 11.0 | 2.10 | 4300 | $b = 8.5$ Å | 0.7 |
| PEA06R | DE | No, $\beta = 1$ | 11.4 | 0.77 | 12.6 | $\alpha = 3.4$ | 1.2 |
| | DECLF | No, $\beta = 1$ | 10.6 | 0.77 | 4000 | $v = 0.01$ | 1.2 |
| | TDD | No, $\beta = 1$ | 11.4 | 0.80 | 2450 | $M_d = 2$ kg mol$^{-1}$ | 1.0 |
| | MML | No, $c_v = 0^b$ | 8.0 | 0.88 | 1750 | $b$, undetectable[c] | 1.0 |
| | DE | Yes, $\beta = 2.1$ | 18.2 | 0.82 | 530 | $\alpha = 3.4$ | 1.1 |
| | DECLF | Yes, $\beta = 2.1$ | 11.5 | 0.80 | 38,800 | $v = 0.1$ | 0.8 |
| | TDD | Yes, $\beta = 2.1$ | 10.5 | 0.85 | 12,000 | $M_d = 14$ kg mol$^{-1}$ | 0.8 |
| | MML | Yes, $c_v = 1^b$ | 9.0 | 0.51 | 5600 | $b = 6.5$ Å | 0.8 |
| PEA20R | DE | No, $\beta = 1$ | 12.1 | 0.85 | 40,700 | $\alpha = 2.8$ | 1.6 |
| | DECLF | No, $\beta = 1$ | 10.0 | 0.80 | 2700 | $v = 0.4$ | 1.4 |
| | TDD | No, $\beta = 1$ | 11.0 | 0.84 | 1600 | $M_d = 0.5$ kg mol$^{-1}$ | 1.0 |
| | MML | No, $c_v = 0^b$ | 8.0 | 0.84 | 980 | $b$, undetectable[c] | 1.6 |
| | DE | Yes, $\beta = 2.1$ | 13.0 | 0.76 | 2.05 | $\alpha = 3.8$ | 1.2 |
| | DECLF | Yes, $\beta = 2.1$ | 11.5 | 0.78 | 38,000 | $v = 0.2$ | 0.8 |
| | TDD | Yes, $\beta = 2.1$ | 10.5 | 0.78 | 127,000 | $M_d = 30$ kg mol$^{-1}$ | 0.8 |
| | MML | Yes, $c_v = 1^b$ | 11.0 | 0.83 | 6200 | $b = 4.5$ Å | 0.8 |

[a] Constrained value

[b] In this case, $\beta$ of Eq. 15 is a dummy variable, to be set to 1

[c] Note that in absence of CR, the MML model reduces to 3 the number of free parameters being $b$ only accounted for in the CR function $R(c_v, t)$

assumptions made about the strength of CR mechanism are confirmed.

Further tests and method analysis

To conclude this study, we further test the possibility of profitably carrying out separate coherent simulations of the PEA samples and we discuss, in comparison, the outcomes of a more straightforward method consisting in a global fitting procedure that includes all the master curves.

Regarding the possibility of carrying out single coherent simulations of the PEA samples in the range of mass from slightly entangled to entangled ones, a graphical method is shown in Fig. 11 to control the quality of the models and to display the validity of our conclusions about the best model for PEAs. The three-variable star plot refers to the parameters of Tables 5 and 7, obtained in the 3 free-parameter simulations with CR mechanism. The standard

deviations of parameters $K_R$ and $M_e$ divided by their mean values are reported over two axes, while the same ratio is calculated for the reptation parameter of the considered model and is reported on the third axis. Note that for the TDD and MML models, there is a separated display for well-entangled ("-1") samples, in the presence of entanglement plateau (PEA06R and PEA20R), and for the remaining ("-2") samples, showing the degree of inability of these models to provide coherent simulations of PEAs in the absence of an evident entanglement plateau.

It is seen that the DECLF model exhibits the less dispersed geometry, as confirmed by the area of the pertinent triangle. This result supports our previous detailed analysis and indicates DECLF as eligible to calculate in a coherent manner the rheological response in the mass range of polymers from slightly to well-entangled regime.

To get more insight into the proposed method of analysis, a multiple curve fit is carried out that simulates the whole
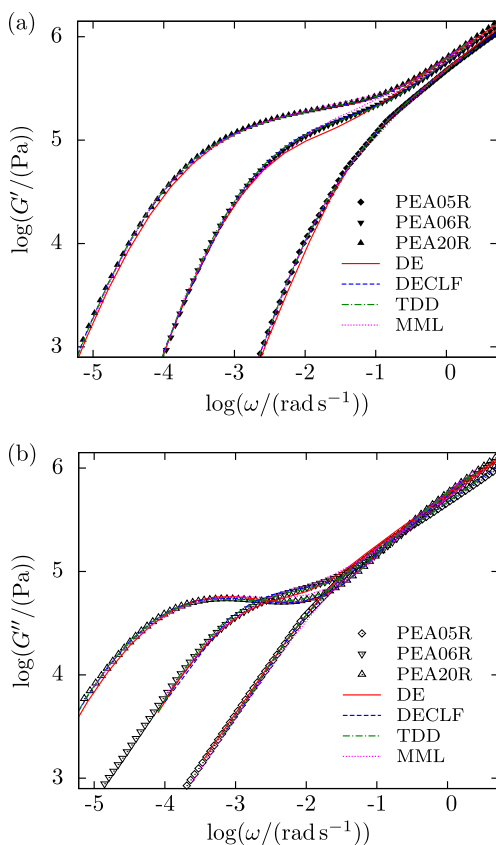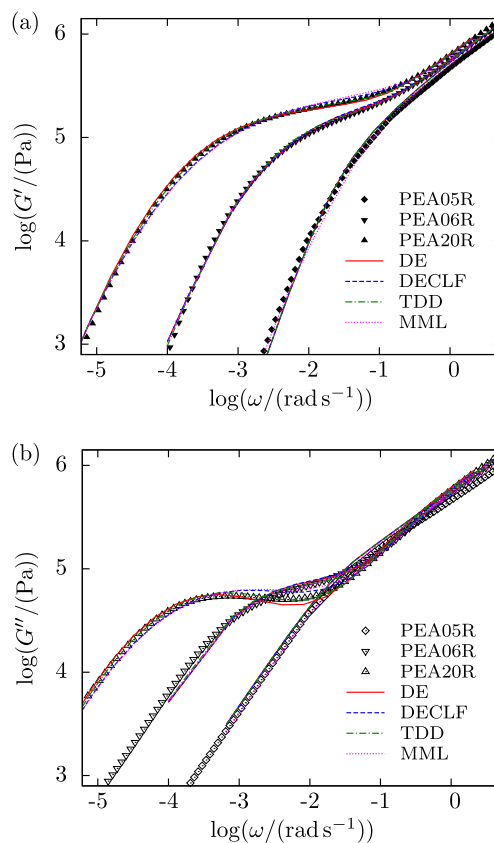
**Fig. 8** Entangled PEA05R, PEA06R, and PEA20R samples: 4 free-parameter reptation models with CR. Experimental master curves and superimposed calculated $G'$ (**a**) and $G''$ (**b**) moduli



**Fig. 9** Entangled PEA05R, PEA06R, and PEA20R samples: 4 free-parameter reptation models without CR. Experimental master curves and superimposed calculated $G'$ (**a**) and $G''$ (**b**) moduli

master curve set by means of a single Nelder–Mead routine. This was accomplished by extension of Eq. 16 to the following cost function:

$$\mu_{\log} = \frac{1}{5}\sum_{i}^{5}\frac{1}{P_i - n}\sum_{k=1}^{P_i}\left(\frac{\log\left(G'_{i\,\exp}\left(\omega_{k,i}\right)/G'_{i\,\text{th}}\left(\omega_{k,i}\right)\right)}{\sigma}\right)^2$$
$$+ \frac{1}{5}\sum_{i}^{5}\frac{1}{P_i - n}\sum_{k=1}^{P_i}\left(\frac{\log\left(G''_{i\,\exp}\left(\omega_{k,i}\right)/G''_{i\,\text{th}}\left(\omega_{k,i}\right)\right)}{\sigma}\right)^2$$

where the index $i$ spans the sample set. We selected a multiple-fitting procedure for DECLF, TTD, and DE models including CR relaxation, where $K_R$, $M_e$, and the reptation parameter appropriate to the model were set as free. This choice is consistent with the conclusion of the previous paragraph, where it has been shown that CR mechanism is effective in the relaxation processes of PEAs and that the 3 free fitting parameter procedures are eligible over those with 4 free parameters.

For the TDD model, $M_e = 17.0$ kg mol$^{-1}$, $K_R = 0.80$ ms, and $M_d = 13$ kg mol$^{-1}$ were obtained, with an overall

$\mu_{\log} = 3.1$. TDD might easily expected to be unsatisfactory because the previous findings, according to the single-fit procedure, provided mass-dependent $M_d$ (see Fig. 11) with incoherent values between the ranges of slightly and highly entangled PEAs. It resulted for DE: $M_e = 15.7$ kg mol$^{-1}$, $K_R = 0.86$ ms, and $K_d/K_R = 330$, with $\mu_{\log} = 2.7$. The DECLF model confirmed itself as the eligible one with the smallest value of $\mu_{\log} = 1.6$. $M_e = 11.8$ kg mol$^{-1}$, $K_R = 0.81$ ms, and $v = 0.2$ are found to be compatible with the values found in single-fitting procedure (Tables 5 and 7).

As a final issue of the present section, the attention is addressed to the form of the cost function. Different choices for it could be adopted. In particular, it has been suggested in the literature a form with the absolute values of the moduli. In Shanbhag (2011), the substantial equivalence of cost functions expressed in terms of logarithms or absolute values was highlighted. In the present study, it has been preferred the logarithmic form (Eq. 16), for its capability to sustain statistical tests.

Nevertheless, with the aim of testing the sensitivity of our conclusions to the alternative definition of the cost function (Shanbhag 2011), a multiple-fitting procedure for DECLF
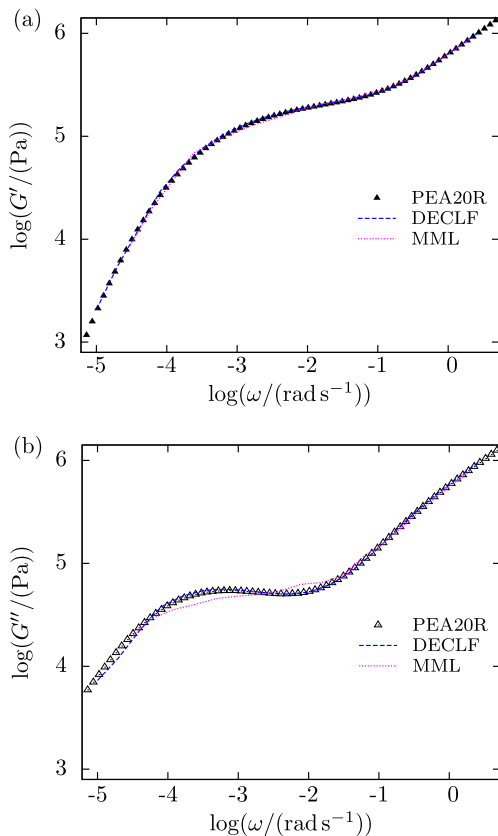
(a)

(b)

**Fig. 10** Calculations of $G'$ (**a**) and $G''$ (**b**) of PEA20R according to the DECLF and MML model with $\beta$ and $c_v$, respectively, used as free, together with $K_R$, $M_e$, and the pertinent reptation parameter of the model
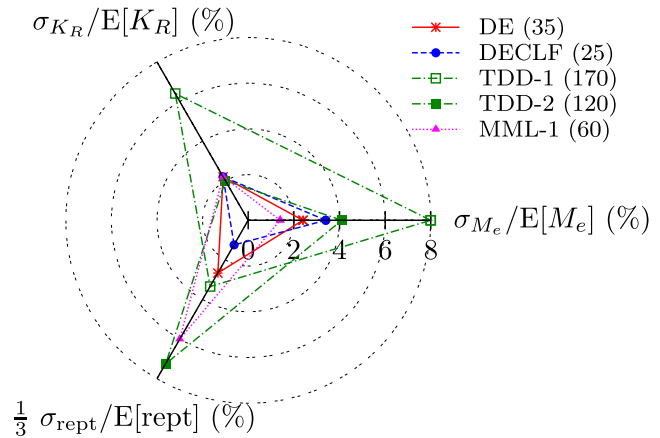


**Fig. 11** Dispersion plots of the fitting parameters obtained in simulations of master curves. The 3 free-parameter case (Tables 5 and 7) with CR is shown. In parenthesis, the area of the triangle (multiplied by $10^4$) is reported. For TDD and MML, samples are collected in two sets on the basis of the presence of the entanglement plateau: "-1" (PEA06R and PEA20R) and "-2" (PEA02R, PEA04R, and PEA05R). MML-1 only is reported in the figure; for MML-2 the area is 0.022 corresponding to the values $\sigma_{M_e}/E[M_e] = 14\,\%$, $\sigma_{K_R}/E[K_R] = 5\,\%$ and $\sigma_{\text{rept}}/E[\text{rept}] = 10\,\%$.

with CR and 3 free fitting parameters has been carried out minimizing the function

$$\mu_{\text{abs}} = \frac{1}{5}\sum_{i}^{5}\frac{1}{P_i - n}\sum_{k=1}^{P_i}\left|\frac{\log\left(G'_{i\,\text{exp}}(\omega_{k,i}) - G'_{i\,\text{th}}(\omega_{k,i})\right)}{G'_{i\,\text{exp}}(\omega_{k,i})}\right|$$
$$+ \frac{1}{5}\sum_{i}^{5}\frac{1}{P_i - n}\sum_{k=1}^{P_i}\left|\frac{\log\left(G''_{i\,\text{exp}}(\omega_{k,i}) - G''_{i\,\text{th}}(\omega_{k,i})\right)}{G''_{i\,\text{exp}}(\omega_{k,i})}\right|$$

The outcome of the procedure provided the following values of the free parameters: $M_e = 12.0$ kg mol$^{-1}$, $K_R = 0.78$ ms, and $v = 0.15$. This result has to be compared with the above values pertinent to the multiple-fitting procedure according to the minimization of $\mu_{\text{log}}$. It is seen that they result in good agreement with each other. A calculation of $\mu_{\text{log}}$ according to the values found at the minimum of $\mu_{\text{abs}}$ gives $\mu_{\text{log}} = 1.9$.

## Entanglement features, packing length, and MML model

The previous study provided a set of information about materials parameters of the PEA polymers that were unambiguously determined. More insight can be gained on PEAs, looking at universal empirical laws that link entanglement parameters, such as $M_e$, and microscopic quantities detailed in literature studies on different polymer melts (Fetters et al. 1994; Fetters et al. 1999).

Accordingly, the packing model is an empirical model and combines entangling properties of the chain with its conformational properties (Fetters et al. 1994; Fetters et al. 1999). All the macromolecular information is contained in the definition of the packing length $\hat{p}$

$$\hat{p} = \frac{M_0}{b^2 N_A \rho} \tag{19}$$

that connects $\hat{p}$ to the effective length $b$ and to the molar mass $M_0$ via the polymer density $\rho$ and the Avogadro number $N_A$. Within the framework of the packing model, the following empirical expression has been developed relating the packing length to the entanglement molar mass (Fetters et al. 1994; Fetters et al. 1999):

$$M_e = 361.9 N_A \rho \hat{p}^3 \tag{20}$$

Starting from the evaluation of $M_e$ for PEAs from Tables 5 and 7, Eq. 20 provides the value of the packing length of the PEA polymers as $\hat{p} = 3.7$ Å, which is analogous to

the one of ordinary flexible polymers (Fetters et al. 1994; Fetters et al. 1999). On the other hand, the effective length $b$ for the PEA can be evaluated from the packing model via Eq. 19, providing $b = 6$ Å, a value nicely similar to that found by the MML calculations reported in this work (Table 7). Then, it is also possible to estimate the Flory characteristic ratio $C_\infty$, defined as the square of the ratio $b/l_0$, where $l_0$ is the length of the dynamic unit along the main chain (Doi and Edwards 1988). It is found $C_\infty = 5.6$, a value similar to literature findings for similar flexible linear homopolymers (Fetters et al. 1994; Fetters et al. 2002).

Information can be obtained also on other molar masses, related to entanglement and reptation, namely the critical mass $M_c$ and the pure reptation mass $M_r$. The pure reptation mass $M_r$ is defined as the molar mass at the crossover between two mass regimes for the viscosity, namely the contour-length fluctuation where $\eta(M) \sim M^{3.4}$ and pure reptation, where $\eta(M) \sim M^3$. Also, at the critical mass $M_c$, the entangled behavior becomes apparent in the materials functions of ordinary flexible polymers (Andreozzi et al. 2006; Fetters et al. 1999; Fuchs et al. 1996), such as the first appearance of the entanglement plateau in $G^*$ master curves. In ordinary entangled polymers, $M_c$ is usually associated to $M_e$ by means of the empirical law $M_c/M_e = 2.0 - 2.2$ and defines the crossover from the Rouse mass dependence of the viscosity to the $M^{3.4}$ regime (Andreozzi et al. 2006; Colby et al. 1987; Ferry 1980). Accordingly, it is possible to write for $\eta(M)$ above $M_c$ (Fetters et al. 1999)

$$\eta(M) = \eta(M_c) \left( \frac{M}{M_c} \right)^{3.4} \qquad (21)$$

Actually, a relationship among $M_c$, polymer molar mass and radius of gyration, was proposed in the literature (Fox and Allen 1964) that can be reformulated in terms of the parameters of the packing-length model as (Fetters et al. 1999)

$$M_c = M_e \left( \frac{9.2\text{Å}}{\hat{p}} \right)^{0.65} \qquad (22)$$

According to Eq. 22, the entanglement and the critical molar mass $M_c$ become equal at $\hat{p} = 9.2$ Å. Adopting the best fit value of the simulation parameters of DECLF model with CR in Tables 5 and 7, Eq. 22 provides $M_c = 22$ kg mol$^{-1}$, which fairly approximates the experimental finding of 26 kg mol$^{-1}$ (Andreozzi et al. 2006). It appears, therefore, that, in this case, a microscopic model, such as the packing length, is able to reproduce via Eq. 22 a fully empirical parameter such as $M_c$. However, if Eq. 21 is rather used together with viscosity data of PEAs reported in Andreozzi et al. (2006), the value for $M_c$ of about 24 kg mol$^{-1}$ is found that fits in a better way the indication drawn in Andreozzi et al. (2006).

Analytically, the reptation mass $M_r$ can be defined as (Graessley 1980, 1982)

$$\eta(M) = \frac{12}{5} \frac{M^3}{M_c M_e^2} \eta(M_c) \qquad (23)$$

$M_r$ signals the crossover from a regime where contour-length fluctuations are active to a pure reptation regime for very long chains, where contribution of the fluctuations is reduced (Doi and Edwards 1988; Likhtman and McLeish 2002) and $\eta(M) \sim M^3$ (Fetters et al. 1999). When $\eta(M_r)$ from Eq. 21 equals $\eta(M_r)$ from Eq. 23, the relationship is found (Fetters et al. 1999)

$$\frac{M_r}{M_e} = 7.17 \left( \frac{M_c}{M_e} \right)^6 \qquad (24)$$

From Eq. 24, the ratio $M_r/M_e$ results to be about 700 if the $M_c/M_e$ value experimentally obtained from Andreozzi et al. (2006) and Eq. 21 are used.

A possible way to verify such finding is done with the calculation of the viscosity curve as a function of the molar mass according to the Rouse model, for oligomers, and MML model for slightly entangled and entangled PEA samples. The MML model is able to provide the crossover of $\eta(M)$ from Rouse to reptation regimes, in an analytical way, without introducing any $M_c$ (Likhtman and McLeish 2002). Very importantly for the consistency of all the results, in the calculation of the viscosity[3], the parameters were set at the average values found in this work for well-entangled PEAs: $c_v = 0.8$, $K_R = 0.70$ ms, $K_d = 4.0$ s (Table 7). Accordingly, $\eta(M)$ was determined as the integral $\int_0^\infty G(t)\, dt$, for PEAs taken in this case as monodisperse homopolymers. The resulting curve is shown in Fig. 12. In the figure (left), a departure from the Rouse behavior at $M_c$, located at about $2M_e$, is apparent, in accordance with the findings of this work and Andreozzi et al. (2006). Also, it is seen the pure reptation region, at sufficiently high molar masses.

This dynamic regime is better appreciated looking at the right side of the Fig. 12, where a rescaled function of the calculated viscosity is plotted as a function of the rescaled mass. Then, the pure reptation region results in a plateau for $\eta/M^3$, at sufficiently high molar masses. Interestingly enough, the plateau onsets at $M_r$ about 8400 kg mol$^{-1}$ that is $\approx 700 M_e$. This value was taken as the intercept of the plateau straight line and the line from the 3.4 power law region, in accordance with the result obtained previously in this work via experimental findings and Eq. 24. In Fig. 12, towards the lowest masses, $M_c$ separates the power law region and the linear dynamic region of the viscosity. This

---

[3]According to the approximations about CR presented in Likhtman and McLeish (2002), it is possible to calculate the viscosity analytically. In such a way, the calculation of $\eta(M)$ depends on $K_R$, $K_d$, $M/M_e$, and $c_v$. It is worth noting that for $Z > 10$ calculations become insensitive to $K_R$.

comparison provides a further confirmation of the predictive ability of the MML model when $K_d$ and $K_R$ are allowed to be uncorrelated and a strong consistency check for the results obtained in the present work.

As a final remark, Fig. 12 also shows the superposition of the rescaled iso-free-volume corrected experimental viscosity of PEA series at 270 K taken from the study of Andreozzi et al. (2006). The agreement of the experimental data with the theoretical values is quite satisfactory.

## Conclusions

It appears of paramount importance for the researcher the availability of coherent values for the quantities and parameters that define the viscoelastic behavior and the microscopic dynamics of relaxation of polymers. Indeed, sometimes, data of the same dynamic parameter, obtained from identical polymer materials but with different molecular weights, exhibit very poor accordance. This is particularly true when the masses of the samples fall in the slightly entangled region. Therefore, with the aim of verifying theoretical models and procedures, different reptation theories were tested in this work on a number of slightly entangled and entangled PEA samples.

Main results can be summarized as follows.

By fitting all the experimental master curves of the shear modulus, it was possible to reach an agreement between the values of $M_e$ obtained from different experiments on the same system and to definitely locate the onset of the entanglement at $M_e$. The onset resulted effective for all the tested models and samples, even if rubbery plateau in $G^*$ and reptation dynamics in the mass dependence of viscosity manifested itself experimentally at molar masses higher than $M_c \sim 2M_e$. Moreover, all the microscopic parameters appear to be each other in a very good agreement, once that all the relevant dynamic processes and mixing rules

were suitably taken into account to model the microscopic dynamics of the polymer series at the different masses.

In our opinion, this result suggests the need of placing the sample in a wider dynamic frame if reliable microscopic dynamic description is requested in the presence of intermediate masses of the polymers at the crossover between unentangled and entangled dynamics.

It is worth noting that, because of the very different tail concentration in the samples, in the present study, "inverse" iso-free-volume correction had to be performed for slightly entangled PEAs in order to fit experimental data and theoretical models. This correction uses a mass dependence function for the WLF $c_1$ parameter inferred in the free-volume framework and effective also in the isofrictional correction of the viscosity (Andreozzi et al. 2006; Andreozzi et al. 2008).

Regarding the dynamic models, we were able to show that all the reptation models provided good results in reproducing the experiments. However, a more refined analysis designated DECLF model, also inclusive of CR relaxation, as the most suitable for modeling the PEAs microscopic dynamics from slightly to highly entangled samples.

According to the present study, the suggested procedure in the presence of slightly entangled polymers foresees the use of reptation models after implementation of the "inverse" isofrictional correction. The transition regime of the masses requires to adopt a simulation strategy sample by sample, looking for the best dynamic model that ensures coherence of the mass independent material parameters such as $M_e$ and $K_R$, rather than a global multiple-fitting procedure that could hide relaxation mechanisms and provide rough values of the materials parameters.

Shear macroscopic response of linear PEA homopolymers and pertinent reptation parameters were also successfully related to the coiling properties of the polymer matrix, according to the packing-length model. We provided estimation of the packing length as well as the Flory

**Fig. 12** Mass dependence of viscosity for PEAs as evaluated according to the Rouse and MML models. Experimental values of the iso-free-volume corrected viscosity $\eta(M)/\eta(M_c)$ of PEAs at the temperatures of 270 K (Andreozzi et al. 2006; Colby et al. 1987) are also superimposed in correspondence of their $M_w$. The rescaled $\eta/M^3$ plot (*right side*) is more effective in highlighting details with respect to the $\eta$ versus $M$ graph (*left side*)
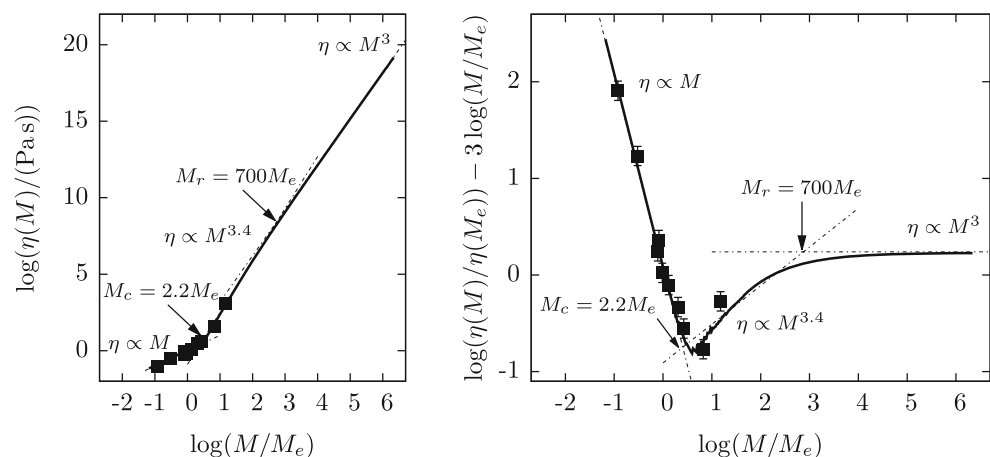
characteristic ratio $C_\infty$ and the effective bond length of PEA homopolymers. All the values resulted in accordance and comparable with the literature ones for similar linear homopolymers. Interestingly enough, it was evidenced the consistence of the value for effective bond length drawn from fitting procedures and the packing-length model, as well as the estimation of the critical mass $M_c$ according to packing model and the experiment. The predictive ability of MML, supported with the best fit values previously obtained for master curves of dynamic moduli, was used in PEAs to infer the critical mass $M_c$ and the pure reptation mass $M_r$.

In conclusion, the analysis of the rheological response in the linear viscoelastic regime in terms of dynamic models represents a powerful investigation tool for the PEA homopolymers, providing unambiguous results for dynamic processes and relaxation mechanisms that take place at the different length scales of the PEAs.

# References

Andreozzi L, Castelvetro V, Faetti M, Giordano M, Zulli F (2006) Rheological and thermal properties of narrow distribution poly(ethyl acrylate)s. Macromolecules 39:1880–1889

Andreozzi L, Galli G, Giordano M, Zulli F (2013) A rheological investigation of entanglement in side-chain liquid-crystalline azobenzene polymethacrylates. Macromolecules 46:5003–5017

Andreozzi L, Autiero C, Faetti M, Giordano M, Zulli F (2008) Dynamics, fragility, and glass transition of low-molecular-weight linear homopolymers. Philos Mag 88:4151–4159

Carrot C, Guillet J (1997) From dynamic moduli to molecular weight distribution: a study of various polydisperse linear polymers. J Rheol 41:1203–1220

Colby RH, Fetters LJ, Graessley WW (1987) The melt viscosity-molecular weight relationship for linear polymers. Macromolecules 20:2226–2237

de Gennes P-G (1971) Reptation of a polymer chain in the presence of fixed obstacles. J Chem Phys 55:572–579

des Cloizeaux J (1988) Double reptation vs simple reptation in polymer melts. Europhys Lett 5:437–442

des Cloizeaux J (1990) Relaxation and viscosity anomaly of melts made of long entangled polymers: time-dependent reptation. Macromolecules 23:4678–4687

des Cloizeaux J (1992) Relaxation of entangled and partially entangled polymers in melts: time-dependent reptation. Macromolecules 25:835–841

Doi M, Edwards SF (1988) The theory of polymer dynamics, 2nd ed. Clarendon Press, Oxford

Ferry JD (1980) Viscoelastic properties of polymers, 3rd ed. Wiley, New York

Fetters LJ, Lohse DJ, Richter D, Witten TA, Zirkel A (1994) Connection between polymer molecular weight, density, chain dimensions, and melt viscoelastic properties. Macromolecules 27:4639–4647

Fetters LJ, Lohse DJ, Milner ST, Graessley WW (1999) Packing length influence in linear polymer melts on the entanglement, critical, and reptation molecular weights. Macromolecules 32:6847–6851

Fetters LJ, Lohse DJ, García-Franco CA, Brant P (2002) Prediction of melt state poly($\alpha$-olefin) rheological properties: the unsuspected role of the average molecular weight per backbone bond. Macromolecules 35:10096–10101

Fuchs K, Friedrich C, Weese J (1996) Viscoelastic properties of narrow-distribution poly(methyl methacrylates). Macromolecules 29:5893–5910

Fox TG, Allen VR (1964) Dependence of the zero-shear melt viscosity and the related friction coefficient and critical chain length on measurable characteristics of chain polymers. J Chem Phys 41:344–352

Graessley WW (1980) Some phenomenological consequences of the Doi–Edwards theory of viscoelasticity. J Polym Sci Polym Phys Ed 18:27–34

Graessley WW (1982) Entangled linear, branched and network polymer systems— molecular theories. Adv Polym Sci 47:67–117

Hiemenz PC, Lodge TP (2007) Polymer chemistry, 2nd. Taylor & Francis, Florida, pp 486–491

Hohne G, Hemminger VF, Flammersheim H-J (2003) Differential scanning calorimetry. Springer-Verlag, Berlin

Honerkamp J, Weese J (1993) A note on estimating mastercurves. Rheol Acta 32:57–64

Ianniruberto G, Marrucci G (1996) On compatibility of the Cox–Merz rule with the model of Doi and Edwards. J Non-Newtonian Fluid Mech 65:241–246

Larson RG, Sridhar T, Leal LG, McKinley GH, Likhtman AE, McLeish TCB (2003) Definitions of entanglement spacing and time constants in the tube model. J Rheol 47:809–818

Larson RG, Zhou Q, Shanbhag S, Park SJ (2007) Advances in modeling of polymer melt rheology. AIChE Journal 53:542–548

Léonardi F, Majesté J-C, Allal A, Marin G (2000) Rheological models based on the double reptation mixing rule: the effects of a polydisperse environment. J Rheol 44:675–692

Likhtman AE, McLeish TCB (2002) Quantitative theory for linear dynamics of linear entangled polymers. Macromolecules 35:6332–6343

Likhtman AE (2014) The tube axis and entanglements in polymer melts. Soft Matter 10:1895–1904

Lin YH, Juang JH (1999) Onset of entanglement. Macromolecules 32:181–185

Liu C, He J, van Ruymbeke E, Keunings R, Bailly C (2006) Evaluation of different methods for the determination of the plateau modulus and the entanglement molecular weight. Polymer 47:4461–4479

Macosko CW (1994) Rheology: principles measurements and applications. Wiley, New York

Marrucci G (1985) Relaxation by reptation and tube enlargement: a model for polydisperse polymers. J Polym Sci Polym Phys Ed 23:159–177

Martinelli L, Baldini L (2008) Misure ed analisi dei dati. ETS, Pisa

Milner ST, McLeish TCB (1998) Reptation and contour-length fluctuations in melts of linear polymers. Phys Rev Lett 81:725–728

Morrison FA (2001) Understanding rheology. Oxford University Press, Oxford

Nelder JA, Mead R (1965) A Simplex Method for Function Minimization. Comput J 7:308–313

Pattamaprom C, Larson RG, Van Dyke TJ (2000) Quantitative predictions of linear viscoelastic rheological properties of entangled polymers. Rheol Acta 39:517–553

Pearson DS, Fetters LJ, Graessley W, Ver Strate G, von Meerwall E (1994) Viscosity and self-diffusion coefficient of hydrogenated polybutadiene. Macromolecules 27:711–719

Richter D, Willner R, Zirkel A, Farago B, Fetters LJ, Huang JS (1994) Polymer motion at the crossover from rouse to reptation dynamics. Macromolecules 27:7437–7446

Rouse PE (1953) A theory of the linear viscoelastic properties of dilute solutions of coiling polymers. J Chem Phys 21:1272–1280

Rubinstein M, Helfand E, Pearson DS (1987) Theory of polydispersity effects of polymer rheology: binary distribution of molecular weights. Macromolecules 20:822–829

Rubinstein M, Colby RH (1988) Self-consistent theory of polydisperse entangled polymers: linear viscoelasticity of binary blends. J Chem Phys 89:5291–5306

Schwarzl FR (1971) Numerical calculation of storage and loss modulus from stress relaxation data for linear viscoelastic materials. Rheol Acta 10:165–173

Shanbhag S (2011) Analytical rheology of branched polymer melts: identifying and resolving degenerate structures. J Rheol 55:177–194

Taylor JR (1997) An introduction to error analysis. University Science Books, Herdon VA

Thimm W, Friedrich C, Roths T, Honerkamp J (2000) Molecular weight dependent kernels in generalized mixing rules. J Rheol 44:1353–1361

Tsenoglou C (1987) Viscoelasticity of binary homopolymer blends. ACS Polym Prep 28:185–186

Tsenoglou C (1991) Molecular weight polydispersity effects on the viscoelasticity of entangled linear polymers. Macromolecules 24:1762–1767

van Ruymbeke E, Keunings R, Stéphenne V, Hagenaars A, Bailly C (2002) Evaluation of reptation models for predicting the linear viscoelastic properties of entangled linear polymers. Macromolecules 35:2689–2699

Viovy JL, Rubinstein M, Colby RH (1991) Constraint release in polymer melts: tube reorganization versus tube dilation. Macromolecules 24:3587–3596

Wen J (1999). In: Mark J (ed) Polymer data handbook. Oxford University Press, Oxford